energies

MDPI

Article

# Techno-Economic Assessment of a Combined Heat and Power Plant Integrated with Carbon Dioxide Removal Technology: A Case Study for Central Poland

**Paweł Gładysz [1,*], Anna Sowiżdżał [2], Maciej Miecznik [3], Maciej Hacaga [4] and Leszek Pająk [2]**

1 Faculty of Energy and Fuels, AGH University of Science and Technology, 30-059 Kraków, Poland
2 Faculty of Geology, Geophysics and Environmental Protection, AGH University of Science and Technology, 30-059 Kraków, Poland; ansow@agh.edu.pl (A.S.); pajakl@agh.edu.pl (L.P.)
3 Department of Renewable Energy and Environmental Research, Mineral and Energy Economy Research Institute of the Polish Academy of Sciences, 31-261 Kraków, Poland; miecznik@min-pan.krakow.pl
4 Faculty of National Security, War Studies University, 00-910 Warszawa, Poland; m.hacaga@akademia.mil.pl
* Correspondence: pawel.gladysz@agh.edu.pl

Received: 5 April 2020; Accepted: 1 June 2020; Published: 3 June 2020


**Abstract:** The objective of this study is to assess the techno-economic potential of the proposed novel energy system, which allows for negative emissions of carbon dioxide ($CO_2$). The analyzed system comprises four main subsystems: a biomass-fired combined heat and power plant integrated with a $CO_2$ capture and compression unit, a $CO_2$ transport pipeline, a $CO_2$-enhanced geothermal system, and a supercritical $CO_2$ Brayton power cycle. For the purpose of the comprehensive techno-economic assessment, the results for the reference biomass-fired combined heat and power plant without $CO_2$ capture are also presented. Based on the proposed framework for energy and economic assessment, the energy efficiencies, the specific primary energy consumption of $CO_2$ avoidance, the cost of $CO_2$ avoidance, and negative $CO_2$ emissions are evaluated based on the results of process simulations. In addition, an overview of the relevant elements of the whole system is provided, taking into account technological progress and technology readiness levels. The specific primary energy consumption per unit of $CO_2$ avoided in the analyzed system is equal to 2.17 $MJ_{LHV}$/kg $CO_2$ for biomass only (and 6.22 $MJ_{LHV}$/kg $CO_2$ when geothermal energy is included) and 3.41 $MJ_{LHV}$/kg $CO_2$ excluding the $CO_2$ utilization in the enhanced geothermal system. Regarding the economic performance of the analyzed system, the levelized cost of electricity and heat are almost two times higher than those of the reference system (239.0 to 127.5 EUR/MWh and 9.4 to 5.0 EUR/GJ), which leads to negative values of the Net Present Value in all analyzed scenarios. The $CO_2$ avoided cost and $CO_2$ negative cost in the business as usual economic scenario are equal to 63.0 and 48.2 EUR/t $CO_2$, respectively, and drop to 27.3 and 20 EUR/t $CO_2$ in the technological development scenario. The analysis proves the economic feasibility of the proposed $CO_2$ utilization and storage option in the enhanced geothermal system integrated with the $sCO_2$ cycle when the cost of $CO_2$ transport and storage is above 10 EUR/t $CO_2$ (at a transport distance of 50 km). The technology readiness level of the proposed technology was assessed as TRL4 (technological development), mainly due to the early stage of the $CO_2$-enhanced geothermal systems development.

**Keywords:** $CO_2$ capture; utilization and storage; combined heat and power; $CO_2$ enhanced geothermal systems; supercritical $CO_2$ power cycles; biomass; negative emission technologies

## 1. Introduction

Over the last two decades, deep changes have influenced the energy sector from both the point of view of energy sources and that of technologies in use. The main factors behind these changes are the pursuit of more sustainable electricity generation, and economic and energy security considerations. Europe is one of the most vivid examples. Some of the European Union member states—for example, Germany—make efforts to be leaders in introducing changes in the energy sector. Human-induced climate change (mainly GHG emissions from various industry sectors) is pushing the pursuit of more sustainable and environmentally friendly electricity generation. There are different pathways, depending on the states' energy and climate policies and conditions to meet this objective. However, some technologies and policy actions are included in all of them, viz. renewable energy sources, energy efficiency, and decarbonisation. In Polish official documents concerning energy policy [1] and pathways for the country's development [2], these mechanisms are also included. The concept analyzed within the paper is coherent with all three points, as it emphasizes the usage of renewable energy sources (by means of biomass and geothermal energy), the increase in energy utilization efficiency (by means of the cogeneration of heat and electricity), and the decarbonisation (by means of $CO_2$ capture, utilisation, and storage) of the energy sector (Figure 1). All of them combined lead to the possibility of obtaining so-called "negative" $CO_2$ emissions and increasing economic profitability as a result of the synergy between those three pillars.

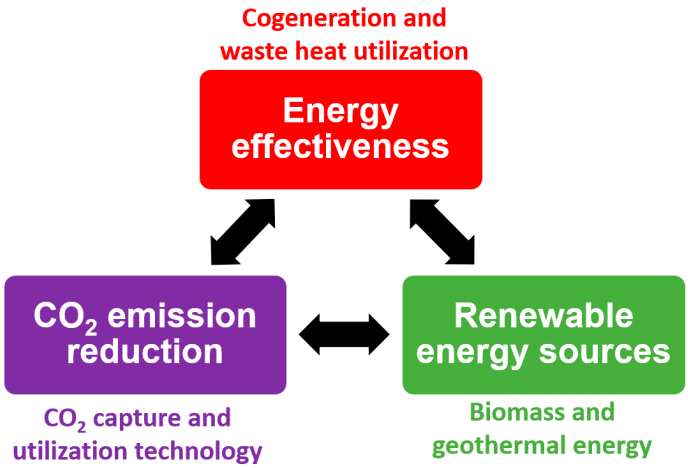


**Figure 1.** Three pillars of new energy systems.

The main goal of this paper is to give a wide overview of the important aspects regarding the proposed system, both from technological and economic points of view. A location in Central Poland was used as a base for a case study, but the presented results can be applied to other locations. However, it should be kept in mind that, e.g., enhanced geothermal system performance is strictly associated with available geological formations. Additionally, the biomass-fired combined heat and power (CHP) plants operating in different countries have different designs depending on the heat demand over the year. In Nordic countries, designs with back-pressure steam turbines are widely used, whereas in other countries (like Poland), extraction-condensing turbines are used more often, and back-pressure turbines are only used at industrial sites with constant heat demand. All of those aspects should be kept in mind when applying the results of this study to other locations and countries. Therefore, we provide a detailed method description for crucial parts of the analysis—carbon dioxide-enhanced geothermal system ($CO_2$-EGS) operation and economic assessment—to allow others to implement the presented concept for their case studies.

### *1.1. $CO_2$ Capture, Utilization, and Storage (CCUS)*

As many countries are failing to meet the Paris agreement climate goals, it becomes more and more obvious that all available technologies must be used to curb emissions. After a period of inattention, government interest in Carbon Capture and Storage (CCS) technology has been rising since 2018 [3]. Its global progress has been monitored on a regular basis by the Global CCS Institute through the Carbon Capture and Storage (CCS) Readiness Index (CCS-RI). It comprises four sub-indicators that track all the necessary aspects of technological development: inherent interest, policy issues, regulatory and legal frameworks, and storage development [4]. Within the group of the high-scoring states, one finds the most developed states, namely Australia, Canada, Norway, the United Kingdom, and the United States. China, Denmark, Germany, Japan, and the Netherlands are well-advanced and progressing in introducing CCS [4]. The third group—moderately performing—consists of predominantly European countries. Poland scored 42 points out of 100 and was therefore added to this group [4] (Table 1).

**Table 1.** Top 10 emissions countries versus top 10 Carbon Capture and Storage (CCS)-ready countries [4,5].

| **Emissions (Mt $CO_2$)** | | **Score in the CCS Readiness Index** | |
|---|---|---|---|
| China | 9839 | Canada | 71 |
| United States of America | 5270 | USA | 70 |
| India | 2467 | Norway | 67 |
| Russian Federation | 1693 | United Kingdom | 65 |
| Japan | 1205 | Australia | 62 |
| Germany | 799 | Netherlands | 54 |
| Iran | 672 | China | 53 |
| Saudi Arabia | 635 | Denmark | 52 |
| South Korea | 616 | Germany | 50 |
| Canada | 573 | Japan | 50 |
| Poland (21st position) | 327 | Poland (15th position) | 42 |

Since the 2015 assessment, Poland's overall score has improved. However, it still continues to remain at an average level. A closer look reveals that an increased score in the storage sub-indicator is responsible for the advance. However, Poland belongs to the group where "most of the storage potential is considered only as prospective resources", and the country's experience is limited [6]. Moreover, no change was noted in the policy and regulatory areas. Poland is especially ill-prepared within the former, achieving a score eight times lower than the leader of the policy indicator index, Norway (7 and 56, respectively) [7]. When the regulatory area is considered, Poland belongs to the middle of Band B, the group of countries where only some laws applicable to the CCS project cycle were introduced. The unchanged position of Poland since 2015 indicates limited legislative activity and policy development [8] (Table 2).

**Table 2.** Poland versus Canada (the leading state) performance comparison.

| **Indicator** | **Canada** | **Poland** | **Poland's Position Change since the 2015 Study** |
|---|---|---|---|
| Total 2018 score (CCS-RI) | 71 | 42 | Up |
| CCS Storage Indicator (CCS-SI) | 98 | 68 | Up |
| CCS Policy Indicator (CCS-PI) | 40 | 7 | No change |
| CCS Legal and Regulatory Indicator (CCS-LRI) | 65.5 | 45 | No change |
| CCS Inherent Interest Indicator (CCS-CI) | 88 | 68 | No change |

According to the most recent reports [9], the global CCS fleet consists of 51 large-scale facilities, with 19 in operation, 4 in construction, 10 in advanced development, and 18 in early development. Geographically, the majority of them are concentrated in North America (47%), followed by China (16%, majority in early development) and the UK (12%, all in early development). Current storage capacity is around 39 million tonnes of $CO_2$ annually, which equals slightly more than 0.1% of global emissions. Although the overall survivability rate of CCS projects is 37%, the number of projects entering the pipeline has increased recently and exceeded the number of those exiting. It has been stressed that the pace of CCS adoption is well below of what is required to meet the Paris Agreement goal of a 2 °C increase. While the building rate should reach the level of 70–100 facilities per year, the actual progress has been only one facility annually in the last decade. The report stresses that technologies for CCS are generally well-established. Therefore, there are policy changes on a monumental scale that are necessary for the successful wide-scale deployment of CCS. These include increasing the number of projects entering the pipeline and their survivability rate, as well as protecting them from short-term political changes.

To stop the process of global warming and simultaneously meet climate goals, global society needs to reach and sustain net zero global anthropogenic carbon dioxide emissions. Moreover, even if the process of warming would be halted, negative emission technologies (NETs), also known as carbon dioxide removal (CDR) technologies, may still be essential to prevent further warming [10]. However, meeting the 2 °C goal is practically impossible without using one of the most crucial NETs—bioenergy with carbon capture and storage (BECCS) [11]. Its crucial role comes from the fact that it allows for the double capture of carbon dioxide. Because of using biomass, which captures $CO_2$ in the process of growth, BECSS seems indispensable, as $CO_2$ is captured for the second time when energy is released. Afterwards, emissions are stored underground. Hence, it can mitigate emissions from other sources as well as those emissions that have already occurred [12]. Three categories of biomass input were analyzed—energy crops, forestry residues, and agricultural residues—for two major applications: large scale electricity generation and biofuel production. Technologically, the highest potential for emission reduction was found in biomass integrated gasification combined cycles (BIGCCs) and a circulating fluidized bed (CFB) [13]. However, economically, the potential of a CFB is 20 times less than that of BIGCCs [13]. Even if burned along with fossil fuels, BECCS ensures a low emission profile [12]. With direct air carbon capture and storage (DACCS), BECSS consists of two NETs with the largest overall $CO_2$ removal potentials, albeit at high cost [11]. The amount of biomass that can be sustainably produced and global storage capacity can also limit the spread of BECCS [13].

Coal's domination in the energy mix inspired Poland's attempts to develop CCS installations. Post-combustion carbon capture was planned for the PGE Bełchatów demonstration project, which was supposed to be run in the 858 MW unit, launched in 2011. The Polish CCS project in Bełchatów, despite receiving a positive assessment from the European Investment Bank and European Commission in the first round of recruitment for the EU's NER 300 program, was withdrawn from the competition in 2011 and canceled in 2013. Although the project could have been built with European funds, it was necessary to involve national funds to run it on an everyday basis, which was not politically feasible [14,15]. Other factors that influenced the project closure decision were high costs, insufficient public acceptance, and the incomplete implementation of the CCS Directive [16]. Not much has changed since then. Although extensive performance assessments were conducted in Poland that showed the suitability of geologic settings, from a legal point of view, storage sites can only be located offshore [17]. The recent governmental assessment was that CCS installations can be competitive only when $CO_2$ emission allowances will exceed EUR 50 per ton [18].

One of the main research concerns regarding BECCS is the assessment of the net negative emission status of the technology. The authors of a review paper on Integrated Assessment Models [19] addressed the main criticism regarding their application for the assessment of bioenergy with CCS. The main finding of the paper was the importance of using other models and analytical approaches to enhance the Integrated Assessment Models' role in mitigation pathway analysis. Similarly, in [20],

the authors addressed the topic of BECCS and identified research priorities and the assessment needed to accelerate the deployment of this technology. Among already widely discussed assessment priorities such as the potential of biomass supply, the authors pointed out the importance of alga biomass studies in terms of economic viability, environmental sustainability, and their inclusion in the value chain of biomass for BECCS.

Regarding techno-economic studies of the BECCS, a few studies can be found that deal with an evaluation of bioenergy with CCS in different sectors. In [21], the authors performed such an analysis for a sugarcane mill located in Brazil. They concluded that $CO_2$ capture at the analyzed plant is technically feasible and that the cost of avoided $CO_2$ emissions was 62 EUR/t $CO_2$, with the potential to decrease to 48 EUR/t $CO_2$ in the case of larger plants and more efficient technologies. Authors often propose merging novel $CO_2$ capture with the BECCS concept. In [22], the results of the techno-economic evaluation of BECCS via chemical looping combustion were presented. The cost of $CO_2$ avoidance was estimated at 150 US$/t $CO_2$, compared with BECCS with post-combustion $CO_2$ capture, at around 200 US$/t $CO_2$. A similar conclusion regarding the superiority of novel $CO_2$ capture technologies (in this case, calcium looping) with BECCS over conventional absorption $CO_2$ removal were also reported in [23].

### *1.2. District Heating Systems in Poland*

In 2017, there were more than 400 heating and heating distribution companies operating in Poland [24]. The total installed capacity of heat production reaches almost 55 $GW_{th}$ with around 240 thousand $TJ_{th}$ delivered to the consumers connected to a district heating system (DHS) in Poland. Almost 54% of all heating companies operate in a DHS smaller than 50 $MW_{th}$. The average share of heat produced in cogeneration is around 61%, but it should be noted that it comes mainly from large heat sources in bigger cities. Coal is a dominant fuel in the production mix for heat in Poland (72%), followed by biomass (7.4%) and natural gas (6.8%) [24]. The average price of heat in Poland is around 9 EUR/GJ and varies depending on whether the fuel is in heat-only boilers or a CHP plant (from lignite, 6.3 EUR/GJ, to coal, 8.8 EUR/GJ, and from biomass, 9.8 EUR/GJ, to light fuel oil, 15.6 EUR/GJ).

In recent years, the Polish heating sector has been struggling with several obstacles of a legislative and economic nature. When large DHSs are concerned, most of them manage the upcoming challenges in an effective and economically feasible manner. Most small DHSs (up to 50 $MW_{th}$) are facing serious challenges, both from economic and environmental points of view. About 80% of DHSs, especially small ones (from 1 to about 100 $MW_{th}$), are inefficient according to the Energy Efficiency Directive [25], which might result in a lack of public aid in the near future. In addition, environmental-driven investments are needed, mainly due to the Medium Combustion Plants (MCP) Directive [26], which is setting emission standards for sulphur dioxide ($SO_2$), nitrogen oxides ($NO_x$), and particulate matter (PM) for combustion plants with a rated thermal input of 1 to 50 $MW_{th}$. A change in fuel structure is also needed, as sources with a thermal input above 20 $MW_{th}$ participate in EU-ETS, and after 2030, the free allowances will be gradually reduced. On the other hand, the demand for heat is decreasing as a result of the thermal modernization of buildings connected to DHSs. All of these points have led to an increase in heat production costs, which might result in the disconnection of consumers from the network and switching to individual heat sources (at the level of building complexes, single buildings, or individual apartments).

Several studies have been published in the last three years regarding the challenges of small DHSs and cooperating heat sources [25–28]. As stressed in most of them, the main chances for the successful transformation of a small DHS lies in cogeneration (which could provide an additional 2–4 $GW_{el}$ of electricity production capacity in the system), the popularization of biomass as a fuel in heat-only boilers and CHP plants, and increases in the energy efficiency of buildings (together with an increased usage of district heating for hot tap water preparation).

### *1.3. Enhanced Geothermal Systems*

Classical geothermal systems are based on mature and well-known technology, enabling the exploitation of water accumulated in hydrogeothermal reservoirs. However, huge geothermal potential is present in bedrock with low permeability, low porosity, and low to medium enthalpy. Enhanced Geothermal Systems (EGSs) are unconventional geothermal systems that make it possible to utilize the geothermal energy accumulated in hot rocks characterized by insufficient or little natural permeability or fluid saturation. This kind of system assumes heat extraction from underground hot dry rock (HDR) by an artificial increase in the hydraulic performance of a geothermal reservoir and then the circulation of a working fluid into it and bringing the heated working fluid to a power plant to generate electricity (Figure 2) [29,30].

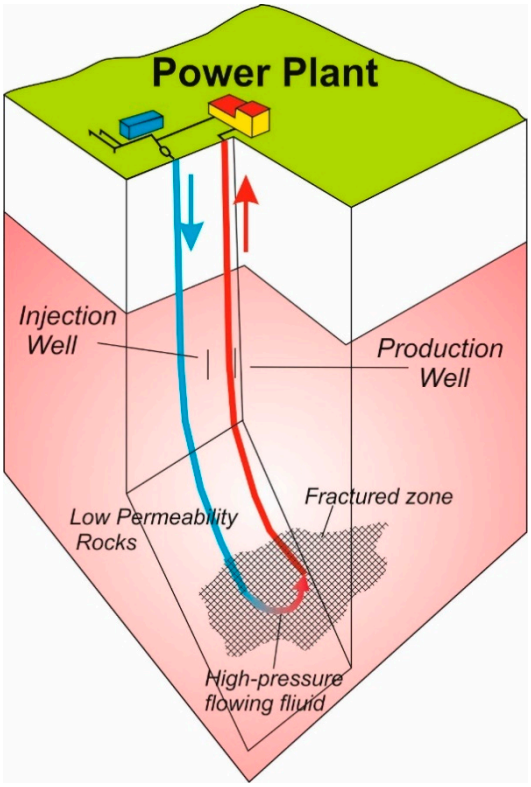


**Figure 2.** Schematic of a conceptual two-well Enhanced Geothermal System (EGS) in hot dry rock (based on [31]).

Conventionally, the only working fluid applied to EGS is water [32]. However, EGS with $CO_2$ as a working fluid is a very attractive option, which results from both energy and environmental benefits. The advantages of this type of solution are due to the more favorable thermodynamic properties of $CO_2$ compared with water, which in turn result in higher production flow rates and reduced carbon emissions into the atmosphere [33–35]. In this case, as the permeability and heat exchange area of the surrounding formation increases, the amount of $CO_2$ sequestration increases too, while the rate of heat extraction decreases slowly, which shows that the permeability of the surrounding formation has a significant impact on $CO_2$ sequestration and the heat extraction rate [36,37].

The concept of $CO_2$-EGS was described for the first time by Brown [38]. This solution appeared as a response to the emerging needs to reduce carbon dioxide emissions in the world. Since then, research has shown a number of advantages of this technology, the basis for which is the possibility of the geological storage of $CO_2$ due to the losses of the working fluid at great depths. However, attention is also paid to other aspects of this solution, including high expansiveness and compressibility, low salt solubility, favorable transport properties, and—due to strong buoyancy—low chemical activity and

self-propelled high flow rates [34,39–41]. For the first time in the world, the EGS has been tested in New Mexico (Fenton Hill). Research conducted since 1974 confirms that such unconventional geothermal systems can work effectively. Since that time, 18 EGS sites have been created around the world, including projects in Australia, Japan, South Korea, German, Sweden, France, Swiss, the UK, and the USA [42]. All current EGS projects use water as a working fluid. An attempt to use $CO_2$ as a working fluid was undertaken in the Ogachi EGS site (1989–2001). The lithological reservoir was granodiorite-characterized by a temperature of more than 230 °C at a 1000 m depth. The large loss of circulating fluid was a limitation to the commercial operation of the system [42]. Currently no EGS-$CO_2$ installation is available. The development of such projects is only at the stage of numerical simulations and laboratory tests [43–45]. However, the results of the conducted research are very promising.

For a comprehensive assessment point of view, the enhanced geothermal systems face some challenges. In [29], the authors proposed a multiple-criteria decision-making approach, which takes technical, geological, economic, environmental, and social impacts into consideration. Proposed within the paper tool is a good example of actions for the support of the wider deployment of the EGS system. The selection methods for power generation in the case of a water-based EGS system have also been discussed in [46], where the authors performed an optimization analysis of single- and double-flash systems, a flash-organic Rankine cycle system, and a double-flash-organic Rankine cycle system. The main findings of the paper indicate that double-flash systems might be a better option for temperatures above 170 °C, whereas a flash-organic Rankine cycle system performs better at lower temperatures. The authors of another study on this subject [30] found similar results regarding the performance of flash systems. In addition, the analyzed expansion-type system proved to have significantly higher geofluid effectiveness than flash-type plants.

### *1.4. Supercritical $CO_2$ Cycles*

The supercritical carbon dioxide (hereinafter referred to as $sCO_2$) cycle was firstly proposed in 1950 [47] and developed in 1967. High thermal efficiency and better temperature glide matching between the heat source and the working fluid are advantages of using $CO_2$ in the supercritical state. It is a machine-friendly (non-corrosive and non-toxic), environmentally friendly, affordable, and accessible working fluid that requires only moderate critical pressure [48]. Amongst the purely practical advantages are the small size of these systems and the wide application possibilities, including in the nuclear, solar, and coal-fired energy industries [47]. The $sCO_2$ cycles receive much interest for applications with waste heat, where a medium to high temperature range is concerned. In [49], the conceptual designs of $sCO_2$ power cycles for such applications were presented. The proposed single flow split with a dual expansion design could provide more than 40% more power compared with a baseline single recuperated cycle. In [50], the authors applied the $sCO_2$ Brayton cycle at a natural gas compression station and compared the selected efficiency indicators with organic Rankine cycles. In addition, as stressed by the authors, when waste heat management is concerned, it is essential to maintain the maximum levels of internal heat recovery and cost-effectiveness.

## 2. Methods

### *2.1. Case Study Selection*

Within the project, for which presented analysis is part of, three scenarios of the modernization of heat sources for small (up to 50 $MW_{th}$) DHSs are considered:

- A reference biomass-fired CHP plant with an extraction-condensing or back-pressure turbine;
- A biomass-fired CHP plant with post-combustion $CO_2$ capture using monoethanolamine (MEA) or calcium-looping processes and storage in saline formations;
- A biomass-fired CHP plant with post-combustion $CO_2$ capture and $CO_2$ utilization via $CO_2$-enhanced geothermal systems.

In this paper, the last option is investigated, viz. a biomass-fired CHP plant with an extraction-condensing turbine, MEA $CO_2$ capture installation, and $CO_2$-EGS utilization. Based on the Polish geological structure analysis and a review of small DHSs, the location in Central Poland was chosen. For the calculation of specific energy consumption for $CO_2$ avoided and $CO_2$ avoided cost (CAC), the results for the reference biomass-fired CHP plant with extraction condensing and without $CO_2$ capture are presented. The design of the reference plant was assumed to provide the same net electrical and heat output as the entire analyzed system.

#### 2.1.1. District Heating System Selection

The demand for heat in municipal district heating systems for the purpose of heating, ventilation, and air-conditioning varies depending on atmospheric conditions. The demand for heat calculations are based on the duration curve of the external temperature in the heating season and the heat demand for hot tap water.

The analyzed DHS plant's main parameters are taken from the available energy plan of the Koło city council [51] and other sources [52,53] and are summarized in Table 3. The analysis within the paper heating network assumes qualitative-quantitative regulations that apply to most of the municipal district heating systems in the world.

**Table 3.** Main parameters of the Koło district heating system (DHS).

| Parameter | Value |
|---|---|
| Climatic zone (in Poland) | II |
| Lowest external temperature characteristic for given climatic zone | −18 °C |
| External temperature when the heating season starts | 12 °C |
| Duration of the heating season | 200 days |
| Maximum heat flux in the DHS | 35,704.4 kW th |
| Maximum heat demand for heating and ventilation in the DHS | 35,150 kW th |
| Hot tap water heat demand in the DHS | 554.4 kW th |
| Temperature of the DHS water output (at maximum heat demand) | 150 °C |
| Temperature of the DHS water input (at maximum heat demand) | 70 °C |
| Temperature of the DHS water (beside heating season, for hot tap water only) | 70 °C/35 °C |

As presented in Table 3, the share of hot tap water in the DHS is very low. The temperatures are also rather high. All those aspects have been raised in the energy plan of the city [51], and suggestions for DHS development over the next years indicate a significant increase in the share of hot tap water in the total heat demand and lowering the DHS temperatures. Taking into account the following remarks, the theoretical DHS was proposed, with a maximum heat demand of 37 $MW_{th}$. For the calculations, the DHS was divided into six zones, where the heat demand and temperatures are presented in Figure 3.

The thermal load of a CHP plant meeting the needs of municipal consumers through the district heating system is characterized by a large degree of irregularity. This is denoted by a considerable ratio of the maximum to the minimum loads (for example, in Poland, the maximum/minimum ratio can reach up to 5:1). The power rating of the turbine (maximum heat production) in a CHP unit must be chosen according to the optimal coefficient of the share of cogeneration, which defines the ratio of the maximum heat flux from the steam turbine (cogeneration) to the maximum demand for heat in the DHS. Based on previous research [52,54,55], an optimal coefficient of the share of cogeneration of 0.6 was assumed in this analysis.

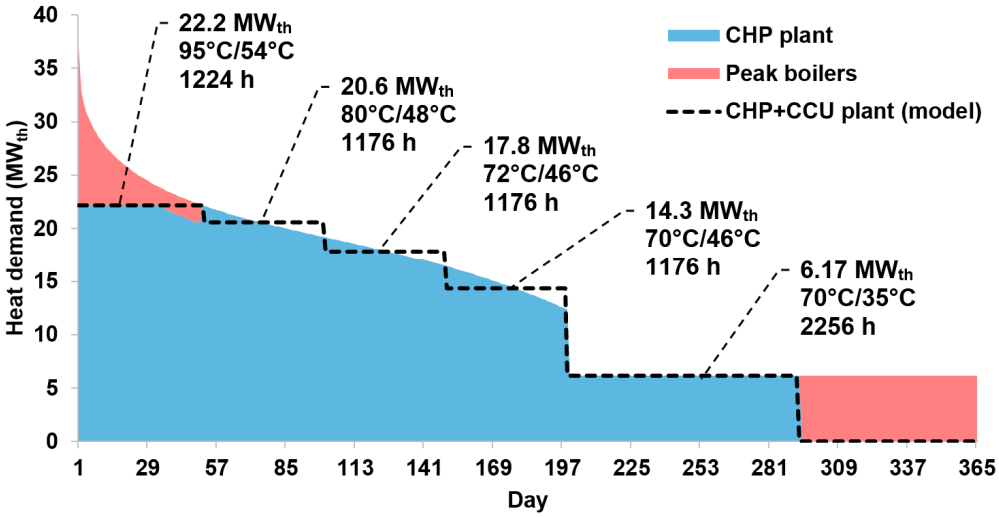


**Figure 3.** Heat demand curve in the analyzed DHS.

Figure 3 presents the duration curve of the demand for heat in the DHS with the area of the operation of the CHP plant and peak boilers. As the gas-fired peak boiler has a minimum operation load of 20%, the decrease in CHP load had to be taken into account. As the availability factor of the CHP plant is assumed at 80%, part of the hot tap water demand (in summer months) is also covered by gas-fired boilers.

### 2.1.2. Geological Structure Selection

The selection of the geological structure is the first and basic element of creating a $CO_2$-EGS system. So far, there is no significant experience in developing such systems, which is reflected in the difficulty of defining the criteria that should be met by a selected geological structure.

Sites prospective for the potential application of an EGS with $CO_2$ as the working fluid ($CO_2$-EGS) should meet the geological and hydrogeothermal conditions suitable for building EGS systems while taking into account the possibilities of the concurrent underground storage of $CO_2$. Sedimentary basins located in tectonically stable areas, with no contemporary volcanism or earthquakes, are best for this purpose [56].

The geological structure designated for underground $CO_2$ storage should form a structural or stratigraphic trap, most favourably in the form of an anticline, characterized by considerable capacity. Reservoir rocks should have an appropriate porosity and permeability to ensure suitable storage capacity, should be tight, should be covered with impermeable rocks with suitable thickness, and should be located at a suitable depth so as to ensure the required pressure and capacity of the $CO_2$ being injected. Rock formations designated for $CO_2$ storage should be located far below any utilized aquifers. They should be separated from them by one or several layers of impermeable insulation rocks, preventing gas from migration to potable water levels that are higher. A degree of isolation of the formations to be used for storage should be considered in relation to the system of hydrodynamic conditions in a given geological structure, trying to control $CO_2$ distribution. A big role is played by the strength of insulating layers, including layer plasticity. They should be thick enough to prevent the phenomenon of fracturing and, in consequence, layer puncture as a result of excessive injection pressure. It is necessary to analyze in detail overlaying sealing beds, which requires detailed studies, tests, and trials. Geological tightness is particularly important, since storage in such structures usually requires higher pressures than hydrostatic pressure. A lack of geological tightness can occur, for instance, in tectonically involved aquifers, which eliminates a given structure for the purposes of carbon dioxide storage [57].

Currently, there is a technological possibility of drilling wells even at depths exceeding 4 km as well as fracturing technology in order to achieve the hydraulic connection between injection and

production boreholes [58]. Therefore, the most suitable rock for EGSs should be characterized by low porosity and permeability values and possibly a high heat flow reflected in a high reservoir temperature. Reservoir rock parameters and sealing rock parameters are both important. In this case, high permeability values may cause an uncontrolled escape of the injected fluid.

Poland is located within three main European geostructural units: the Precambrian East European Platform in the east, which is a large and flat area covered by sediments; the Paleozoic Platform, which comprises the southwestern half of the Polish territory; and the Carpathians, which is a part of the Alpine–Himalayan system in the south. This geostructural position influences the development of the thermal and geological conditions. Most of Poland is covered by sedimentary rocks (Polish Lowlands, Carpathians, and Carpathian Foredeep). The only exception is the Sudetes region (SW part of Poland), where crystalline rocks occur [59].

Geothermal installations currently operating in the area of the Polish Lowlands utilize successfully waters from the Lower Cretaceous and Lower Jurassic reservoirs [60] (Figure 4). It is thus a key premise to treat these reservoirs only as geothermal reservoirs. The situation is different in the case of a Lower Triassic reservoir. All studies conducted so far [61,62] point out the rather poor water content in this reservoir and the low potential for building conventional geothermal installations. Although a EGS geothermal system with a location in a zone of sedimentary rock occurrence shows slightly poorer thermal parameters than systems in crystalline or magma rocks, from the point of view of $CO_2$ sequestration, the best solution is to select sedimentation basins located in tectonically stable areas, which is proven by the above-shown criteria. Due to the depth and expected thermal and petrophysical parameters of Lower Triassic formations, the Krośniewice-Kutno area (Central Poland) was chosen as an optimum location (Figure 4). In this area, the most prospective horizon for an EGS location is the clastic deposits of the Lower Triassic. The top of the reservoir of more than 1000 m thick is behind at depths 5000–5500 m below sea level, and the temperature within the reservoir is in the range 165–195 °C. The porosity of the reservoir rocks is approximately 2.5%, while the permeability is about 0.1 mD [61,63–66].

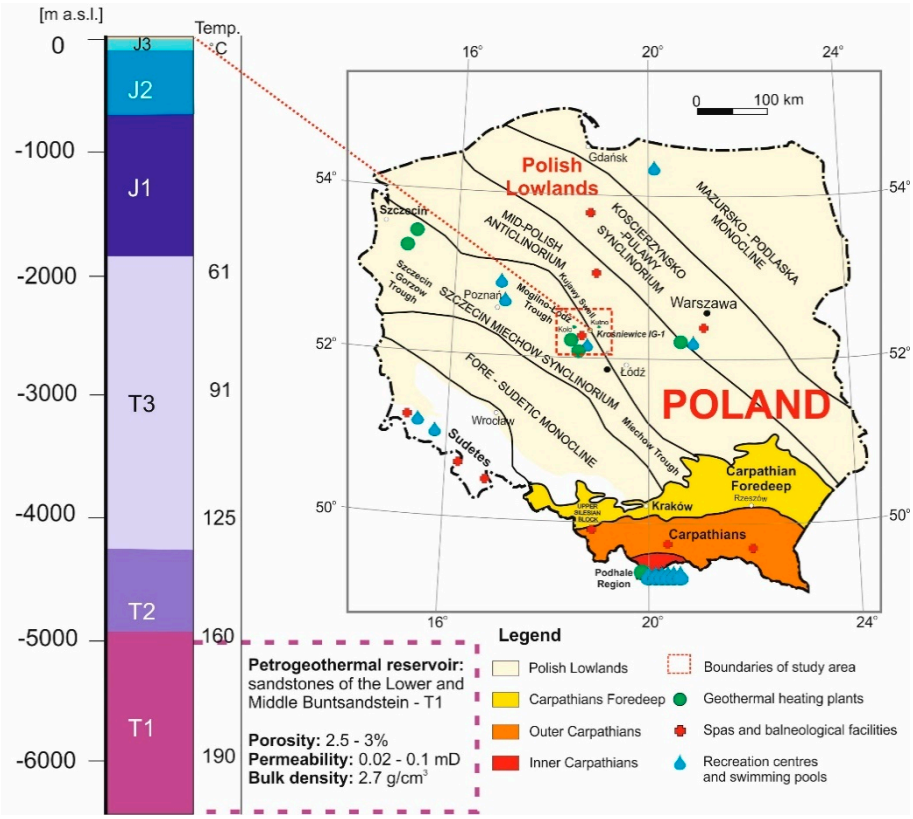


**Figure 4.** Location of the research area together with the predicted geological profile of Krośniewice IG-1.

The estimation of the amount of $CO_2$ that will be permanently bound in the geological structure is a very challenging task. Nevertheless, it can be assumed that this amount will depend on parameters such as the area of major flow paths and the contact area between the fluid and the fractures, the shape of the fractures and their hydraulic connectivity, the porosity and permeability of the geological formation, the reservoir pressure and background pore pressure, the reservoir temperature, the degree of pore saturation with individual fluids, pore fluid phases, and time [62]. The mineralogical composition of the reservoir rocks and the chemical composition of the primary pore fluid will also play important roles in the context of solubility and mineral trapping.

It is estimated that, for the long-term operation of EGS installations with $CO_2$ as a working medium, the amount of stored $CO_2$ is in the order of 5% [34]. However, for different reservoir conditions, the amount of $CO_2$ stored may be different, such as in the case of the geothermal field in Habanero (Australia), where this value seems to be much overestimated [63]. A more precise and site-specific estimation of the amount of $CO_2$ to be stored in the enhanced geothermal reservoir can be achieved with the aid of a numerical simulator coupling heat and mass transport with the reactive geochemistry of fluid–rock interactions [63].

### 2.2. Process Synthesis and Design

The goal of this paper was to model (including the off-design operation) and analyze the full chain of the proposed technology. Thus, the mathematical models of the $CO_2$-EGS (developed in VBA Excel) and the integrated biomass-fired CHP plant with $CO_2$ capture (developed in IPSE Pro) were developed and combined through PSE Excel (a dedicated tool for Excel and IPSE Pro model combinations). A simplified diagram of the analyzed system is presented in Figure 5.

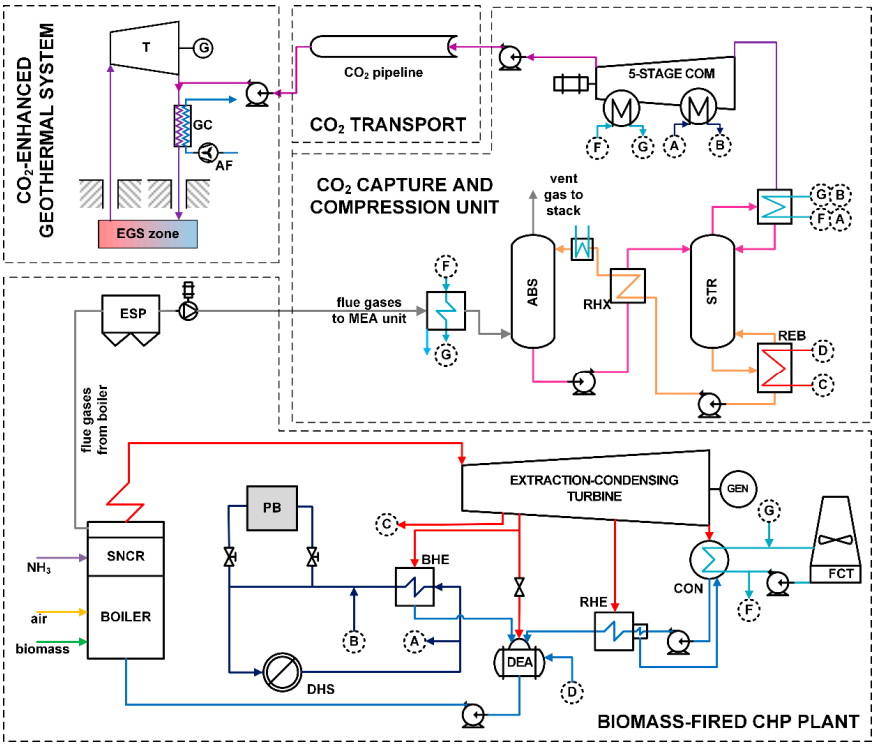


**Figure 5.** Simplified diagram of a CHP unit with an extraction-condensing turbine, a $CO_2$ capture and compression unit, and a $CO_2$-enhanced geothermal system with a supercritical $CO_2$ ($sCO_2$) Brayton cycle (T: turbine; GC: gas cooler; AF: air fan; G: generator; COM: compressor; REB: reboiler; STR: stripper; ABS: absorber; ESP: electrostatic precipitator; BHE: base heat exchanger; RHE: regenerative heat exchanger; FCT: force-draft cooling tower; CON: condenser; DEA: deaerator; PB: peak boiler; SNCR: elective non-catalytic reduction).

In general, the analyzed system can be divided into four main subsystems: (i) a biomass-fired combined heat and power plant integrated with (ii) a $CO_2$ capture and compression unit, (iii) a $CO_2$ transport pipeline, and (iv) a $CO_2$-enhanced geothermal system comprising a geological reservoir and an $sCO_2$ Brayton power cycle. The heat demand in the DHS is covered by the steam extracted from the turbine and the waste heat coming from the $CO_2$ capture and compression unit (mainly the interstage cooling of the $CO_2$ compressors). The cooling duty for the steam condenser in the CHP plant and the $CO_2$ capture and compression unit is achieved by the forced-draft cooling tower. The flue gases after conditioning are directed to the absorber, where $CO_2$ is captured in an amine solution and then released in the stripper. The MEA regeneration is done in the reboiler, where the heat is provided from the steam turbine bleeding. Captured $CO_2$ is then compressed and transported via the $CO_2$ pipeline to the storage (utilization) site. Due to the small range of the $CO_2$ transport (50 km), the rebooster station is not included. The $CO_2$ stream at the EGS site coming from the pipeline is mixed with the circulating stream of $sCO_2$ and injected into the fractured EGS zone, where it heats up. Part of the injected $CO_2$ is sequestrated in the EGS zone (5%), and the rest is directed to the $sCO_2$ turbine. After the turbine, the $CO_2$ is cooled in the gas cooler to the desired temperature. Due to the thermosiphon effect, no additional $CO_2$ compression is needed, as the pressure outlet from the turbine is chosen to utilize the positive pressure difference between the injection and production wells. The amount of $CO_2$ coming from the $CO_2$ capture unit is assumed to be the same as the amount of $CO_2$ sequestered, allowing the system to operate constantly.

#### 2.2.1. Analytical Model of the $CO_2$-Fed Enhanced Geothermal System ($CO_2$-EGS) in the Krośniewice-Kutno Area

Analytical models can be an alternative to detailed 3D numerical models when it is necessary to quickly estimate geothermal reservoir exploitation parameters. As some authors have pointed out [67–69], the 1D and 2D analytical models can often provide a good approximation for more detailed 3D models. Using this approach, a steady-state analytical model of single-channel flow in the EGS reservoir was developed. The model simulates the injection of $sCO_2$ into the fractured zone of the originally low-permeable rock formation, the 1D flow between the injection and production boreholes, and the $CO_2$ extraction using the production well (Figure 6). The assumptions of this model also include laminar (Darcy) flow in the reservoir and turbulent flow in both wells. The temperature of the injected fluid is assumed to linearly increase from the injection zone, to reach a natural reservoir temperature at the feed zone of the production well. The extraction of $CO_2$, the carrier of geothermal heat, can be accomplished either using down-hole pumps or spontaneously, thanks to the thermosiphon effect (similar to the artesian outflow in water wells). Contrary to models developed earlier [66,68,69], the one used here accounts for the heat transfer between $CO_2$, the wells' casings, and the surrounding rocks. A list of the governing equations in this model is given in Appendix A.

The simulation of the $CO_2$ injection into the Lower Triassic sandstones in the Krośniewice-Kutno area was performed for hundreds of different scenarios, in which the thermosiphon effect usually occurs. The two factors that affect the pressure difference between the production and injection wellheads (thermosiphon) the most are the fractured zone permeability and the working fluid ($CO_2$) mass flow rate. For a given mass flow rate and with other parameters kept constant, permeability controls the pressure distribution in the reservoir, affecting the value of thermosiphon (Figure 7). At a certain value of EGS reservoir permeability, a break-even point is reached, and a further increase in permeability does not significantly affect the pressure difference between the production and injection borehole wellheads. What is worth noticing is the fact that, at high reservoir permeability, the thermosiphon process approaches a certain value, regardless of the mass flow rate. As the model couples reservoir and wellbore processes, these results imply that a reservoir pressure drop has a more profound effect than a pressure drop in the wellbore.

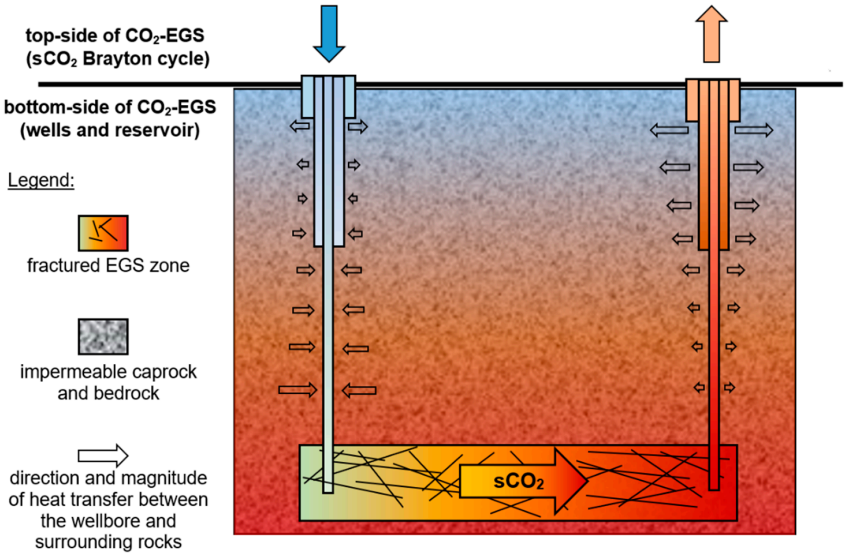


**Figure 6.** Schematic drawing of the single-channel EGS model.

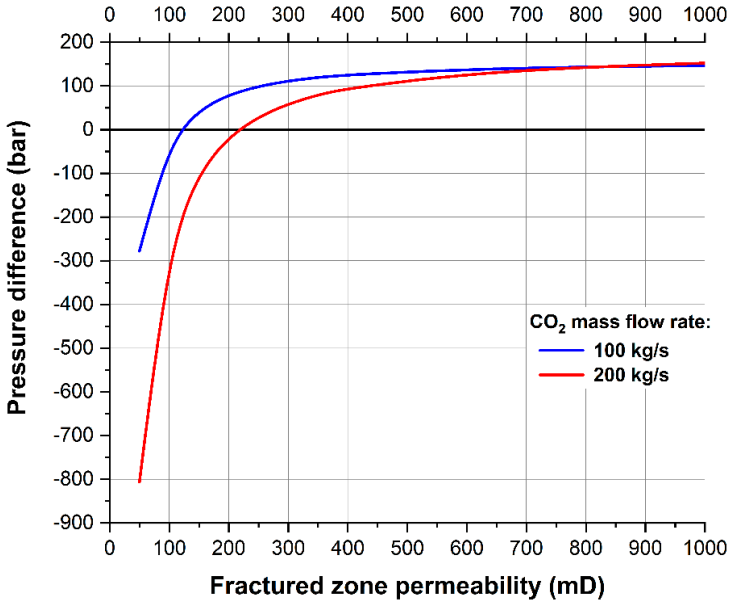


**Figure 7.** The impact of fractured zone permeability on the thermosiphon effect for simulated operating conditions in the Krośniewice–Kutno area (reservoir temperature: 170 °C; reinjection temperature: 35 °C; well depth: 5600 m b.g.l.; wells' separation distance: 600 m; wells casing roughness: 0.04 mm; $CO_2$ sequestration rate: 5%).

### 2.2.2. The CHP Plant with $CO_2$ Capture and $sCO_2$ Brayton Cycle

Based on the analyses concerning the optimal coefficient of the share of cogeneration in DHSs [54] and available data concerning Polish DHSs [24], the coefficient of the share of cogeneration for the analyzed referenced biomass-fired CHP plant is assumed as 0.60, which corresponds to the maximum heat flux for the CHP plant equal to ca. 22.2 $MW_{th}$. In order to meet the maximum heat demand, the peak boilers have to be taken into account (gas-fired units are assumed). The analyzed plant uses a stoker-fired boiler, which burns wood chips with a high moisture content (the $LHV_{ar}$ was around 9534 kJ/kg). Primary steam (53 bar/480 °C) is generated in the boiler and then enters the steam turbine. Steam is extracted at low pressure supplying the regeneration system, which consists of a regenerative heat exchanger preheating the condensate prior to feeding it to the deaerator. Feedwater, after removing oxygen and other dissolved gasses, is pumped into the boiler to repeat the cycle.

The outlet steam (0.04 bar) goes to the heat condenser. Base heat exchangers cover the basic heat demand, resulting from the characteristics of the district heating network, and are supplied with the steam extracted at intermediate pressure (1.9 bar). Part of the heat for the DHS is supplied from the interstage cooling of the $CO_2$ compressors. The same heat extraction from the steam turbine is also used to feed the deaerator after the pressure-reduction valve. The peak heat demand is covered by the gas-fired boilers. The CHP is equipped with the forced draft cooling tower that provides the cooling duty for the condenser, $CO_2$ capture installation, and the interstage cooling of the $CO_2$ compressors. Flue gases from the pulverized biomass boiler are fed into the flue gas conditioning system with selective non-catalytic reduction and an electrostatic precipitator. Due to the low sulphur content in the fuel, the desulphurization system is neglected.

Furthermore, the flue gases are directed to the MEA $CO_2$ capture installation, where the $CO_2$ is captured from flue gases. A $CO_2$ capture efficiency of 90% and a high purity (99.5%) are assumed. The unit heat consumption is calculated based on the approach presented in [70] and is around 3.36 MJ/kg $CO_2$. The saturated steam for the regeneration of the solvent is provided by the extraction of the steam turbine (2.75 bar). Furthermore, the captured $CO_2$ is directed to the $CO_2$ compression train, which comprises five $CO_2$ compressors with interstage cooling (to 30 °C) and a pump that compresses the $CO_2$ to 130 bar. The $CO_2$ is transported via a pipeline for 50 km to the utilization site, where it is compressed to the required pressure of the injection well. It was assumed that 5% of the circulating $CO_2$ is sequestrated, which results in ca. 150 kg/s of $CO_2$ being constantly injected into the geological reservoir. Due to the effect of $CO_2$ thermosiphon, there is no need to add the $sCO_2$ compressor for the remaining mass flow. After the turbine, the $sCO_2$ is cooled down in a gas cooler and is directed to the mixer and then to the injection well. The turbine pressure outlet is determined by the required pressure at the inlet of the injection well plus the pressure loss in the gas cooler [66].

The detailed results regarding the energy performance of the CHP plant, $CO_2$ capture installation, the geological reservoir, and the $sCO_2$ cycle can be found in the previous papers of the authors [55,66,71].

### 2.3. Thermodynamic Assessment

For the purpose of the analysis, the gross and net biomass energy utilization factors (BEUFs) and electrical efficiencies (BEEEs) have been defined as follows, respectively:

$$\eta_{BEUF} = \frac{E_{el} + Q_{DHS}}{E_{ch,bio}} \quad (1)$$

$$\eta_{BEEE} = \frac{E_{el}}{E_{ch,bio}} \quad (2)$$

where $E_{el}$ is the annual electricity production of the system, $Q_{DHS}$ is the annual heat production for the DHS, and $E_{ch,bio}$ is the annual chemical energy of the biomass.

As presented in Equations (1) and (2), the geothermal energy coming from the hot dry rocks is neglected, as the utilization of the geothermal energy is a by-product of the $CO_2$ storage. On the other hand, the electricity production in the $sCO_2$ cycle is included in the annual electricity production. The same approach was applied for the calculations of specific energy consumption for $CO_2$ avoided (SPECCA), where only the biomass chemical energy is considered.

### 2.4. Economic Assessment

Within the economic assessment of the proposed system, both the Levelized Cost of Electricity (LCOE) and that of Heat (LCOH) are calculated. In addition, the Net Present Value (NPV) analysis is performed, including the Break-Even Points (BEP) of negative $CO_2$ emission credits, electricity, and heat.

Both the LCOE and LCOH are aggregated indicators of the costs of the whole process during the system's assumed lifetime. They comprised total investment costs, operational costs (both fixed

and variable), and the obtained electricity or heat production. In this study, the LCOE and LCOH are defined as follows:

$$LCOE = \frac{\varepsilon_{B,el} \times (TSC \times f_a + \sum_i OPEX_i)}{E_{el}} \quad (3)$$

$$LCOH = \frac{\varepsilon_{B,Q} \times (TSC \times f_a + \sum_i OPEX_i)}{Q} \quad (4)$$

where $TSC$ is the Total System Cost (EUR), $f_a$ is the discount factor, and $\sum_i OPEX_i$ is the sum of the variable and fixed operational costs. $\varepsilon_{B,el}$ and $\varepsilon_{B,Q}$ are the total system cost multipliers, which in accordance with the assumed exergy allocation methodology [72] allow the specific costs to be assigned to electricity and heat production. The calculation of the total system cost multipliers relies on the exergy allocation methodology, which takes into account the exergy of useful products in multi-generation processes. For the analyzed system, they take the values of 0.89 and 0.11 for electricity and heat, respectively, and are calculated as follows:

$$\varepsilon_{B,el} = \frac{E_{el}}{E_{el} + \sum_{i=1}^{7008}\left(Q_{DHS,i} \times \frac{T_{m,i}-T_0}{T_{m,i}}\right)} \quad (5)$$

where $T_m$ is the logarithmic mean temperature difference in the DHS, $T_0$ is the reference temperature, and $\varepsilon_{B,Q}$ can be calculated as $1 - \varepsilon_{B,el}$.

Furthermore, within the economic assessment of the proposed systems, the NPV was proposed to incorporate all the sources of potential income (e.g., the negative $CO_2$ emission credits). The NPV is calculated based on the following formula:

$$NPV = \sum_{\tau=0}^{n} \frac{CF_\tau}{(1+r)^\tau} - TSC \quad (6)$$

where for $\tau \geq 1$, the cash flow ($CF_\tau$) is defined as

$$CF_\tau = E_{el} \times c_{el} + Q \times c_{DHS} + G_{CO2} \times c_{CO2,NEC} - \sum_i OPEX_i - TAX \quad (7)$$

where $c_{el}$, $c_{DHS}$, and $c_{CO2,NEC}$ are the prices of electricity, district heat, and negative $CO_2$ emission credits; $r$ is the discount rate; and TAX is the income tax.

The CAC is calculated using the "net present value" method [73], due to the multiple products of the analyzed system (heat and electricity). Necessary assumptions for the validity of the method have been considered, viz. the same net electricity and heat production for the analyzed system with CCS and the reference one. Thus, the CAC is calculated as follows [73]:

$$CAC = \frac{NPV_{CCS} - NPV_{ref}}{\sum_{\tau=0}^{n} \frac{G_{CO2,ref}}{(1+r)^\tau} - \sum_{\tau=0}^{n} \frac{G_{CO2,CCS}}{(1+r)^\tau}} \quad (8)$$

where $G_{CO2}$ is the annual $CO_2$ emissions into the atmosphere.

In addition to the $CAC$, the $CO_2$ negative emission cost (CNC) is proposed, which is defined as follows:

$$CNC = \frac{NPV_{CCS} - NPV_{ref}}{\sum_{\tau=0}^{n} \frac{G_{CO2,neg}}{(1+r)^\tau}} \quad (9)$$

where $G_{CO2,neg}$ is the annual negative $CO_2$ emissions in the analyzed CCS system.

#### 2.4.1. Methodology for Investment Cost Estimation

For each component of the analyzed system, the cost was estimated according to a bottom-up approach where the plants' (the CHP plant, the $CO_2$ capture and compression unit, and the $sCO_2$ power plant) costs were broken down. This allowed for an estimation of the Total System Cost (TSC), which is the sum of the total cost of the subsystems. Each subsystem's total cost was calculated as the Total Equipment Cost (TEC) of the included components and the direct and indirect costs (labor, engineering, integration, etc.). Thus, the TSC of the analyzed system can be defined as follows:

$$TSC = \left\{ \sum_{j} \left(1 + i_{LC,j} + i_{E\&PC,j}\right) \times \left[ \left(1 + i_{P\&C,j}\right) \times \sum_{i} TEC_{i,j} \right] \right\} + TSC_{pipeline} + TSC_{EGS} \quad (10)$$

where $i_{LC}$ is the labor cost indicator, $i_{E\&PC}$ is the engineering and project cost indicator, and $i_{P\&C}$ is the piping and integration cost indicator.

The methodology of the $TEC_i$ calculations for the machinery and equipment, as well as the $TSC$ for the $CO_2$ transport pipeline and the enhanced geothermal system, is presented in Appendix B. The TEC of the CHP plant components was estimated based on [74]. The TEC estimation of the $CO_2$ capture and compression unit follows the guidelines presented in [70] and the reference values obtained from [75]. The TEC of the $sCO_2$ cycle components was estimated based on [76], and the auxiliary equipment's TEC was estimated based on [77]. For the $CO_2$ pipeline, the total subsystem cost was taken from [78], and the data regarding Polish geological locations, for the development of the EGS system, were assumed based on [79]. The formulas presented in Appendix B were adopted, by means of the Chemical Engineering Cost Index [80] and the EUR/USD exchange rates, to EUR in 2017 from their origin years and currencies.

In Table 4, a list of all the equipment that was part of the Total Equipment Cost assessment is presented, taking into account the proposed methods and division into subsystems (Figure 5). The methods for cost calculations are presented in Appendix B.

**Table 4.** List of equipment considered in the investment cost assessment (MEA: monoethanolamine; $sCO_2$: supercritical $CO_2$).

| Subsystem | Equipment and Costs |
| --- | --- |
| Biomass-fired CHP plant | • biomass receiving and preparation infrastructure<br>• biomass grate boiler<br>• extraction-condensing steam turbine<br>• condenser<br>• main heat exchanger (for DHS)<br>• regenerative heat exchangers<br>• deaerator<br>• air fan and flue gas blower with electric motor<br>• pumps with electric motor<br>• electrical generator<br>• force-draft cooling tower<br>• steam extraction (for MEA regeneration) |
| $CO_2$ capture and compression unit | • direct contact cooler<br>• absorber and regenerator (stripper)<br>• rich/lean regenerative heat exchanger<br>• reboiler<br>• MEA reclaimer<br>• solvent processing area<br>• flue gas blower with electric motor<br>• $CO_2$ drying and compression unit (as whole) |

**Table 4.** *Cont.*

| Subsystem | Equipment and Costs |
| --- | --- |
| $CO_2$ transport | • 50 km $CO_2$ pipeline (as whole) |
| $CO_2$-enhanced geothermal system | • $sCO_2$ turbine<br>• $sCO_2$ heat exchanger (gas cooler)<br>• air fan with electric motor<br>• electrical generator<br>• wells and casting<br>• well drilling and EGS zone stimulation |

#### 2.4.2. Financial Assumptions and Scenario Definition

Three scenarios were proposed for analysis within the economic assessment:

- Business as usual, based on the current market in Poland;
- The investment subsidy scenario, where 50% of the investment cost is subsidized by the state (which is a common practice in relation to biomass CHP plants and geothermal installations [79]);
- Technological development, where a 30% decrease in the total systems cost occurs (e.g., due to the technological development in the field of $CO_2$ capture or $sCO_2$ cycle construction—first of a kind vs. nth of a kind).

In Table 5, a summary of financial assumptions is presented for all three analyzed scenarios. In addition, a tax rate of 19% is assumed, together with a 5% depreciation charge for equipment and machinery. The year-by-year changes in heat demand or the parameters of $CO_2$-EGS were neglected in the study.

**Table 5.** Summary of financial assumptions.

| Parameter/Scenario | Business as Usual | Investment Subsidy Scenario | Technological Development |
| --- | --- | --- | --- |
| Location basis | | Central Poland | |
| Cost year basis | | 2017 | |
| Base currency used | | EUR (Euro) | |
| Investment lifetime | | 30 years | |
| Capacity factor | | 80% (7008 h per year) | |
| Discount rate | 10% | 8% | 8% |
| Investment cost | | according to Equation (3) | −30% |
| Subsidies (state grant) | 0% | 50% | 0% |
| Fuel (biomass) cost | | 6 EUR/GJ | |
| OPEX cost: | | | |
| Biomass-fired CHP plant | | 3.2% of CAPEX | |
| $CO_2$ capture and compression unit | | 2.5% of CAPEX | |
| $CO_2$ transport pipeline | | 0.1% of CAPEX | |
| EGS wells | | 0.1% of CAPEX | |
| $sCO_2$ power plant | | 3.0% of CAPEX | |
| Electricity price | 100 EUR/MWh | 50 EUR/MWh | 100 EUR/MWh |
| Heat price | | 10 EUR/GJ | |
| $CO_2$ credit (negative emission credit) * | | 20 EUR/t $CO_2$ | |

* $CO_2$ credit for negative emissions was assumed as the equivalent of the EU-ETS emission allowance.

Regarding the assumption in each scenario (Table 4), the discount rate decrease by 2 percentage points in the subsidy and technological development scenario is mainly due to a lower project risk. The electricity price in the subsidy scenario decreases to average market prices in Poland, as state support for the investment cost is assumed. In other scenarios, the RES support scheme deployed in Poland was taken into account, which predicts a maximum price of 440 PLN/MWh (ca. 105 EUR/MWh)

for the biomass-based and geothermal electricity production. In the current legal system in Poland, a feed-in tariff for electricity and subsidy grants for investment costs exclude each other to a large degree due to the legal regulations that state that if an investment grant is higher than the total feed-in tariff subsidy (over 15 years) for electricity, then further state support cannot be granted.

## 3. Results

### 3.1. Energy Balance

In Table 6, a summary of results regarding the annual operation of the analyzed system is presented.

**Table 6.** Summary of the energy and environmental analysis.

| Parameter | Analyzed System * | Reference CHP Plant |
|---|---|---|
| Gross electricity production: | | |
| in a steam turbine generator | 130,157.1 MWh/a | 121,372.8 MWh/a |
| in an $sCO_2$ Brayton turbine generator | 23,102.8 MWh/a | - |
| Electricity own consumption: | | |
| in a CHP plant | 6157.3 MWh/a | 4758.2 MWh/a |
| in a $CO_2$ capture and compression unit | 27,470.3 MWh/a | - |
| in an $sCO_2$ Brayton cycle | 3017.7 MWh/a | - |
| **Net Electricity Production of the System** | **116,614.6 MWh/a** | |
| **Heat Production to DHS (Total)**, incl.: | **371.3 $TJ_{th}$/a** | |
| steam turbine extraction | 283.6 $TJ_{th}$/a | 371.3 $TJ_{th}$/a |
| interstage cooling of $CO_2$ compressors | 87.7 $TJ_{th}$/a | - |
| Heat production for MEA regeneration | 697.6 $TJ_{th}$/a | - |
| Energy input, incl.: | | |
| **chemical energy of biomass** | **2124.6 $TJ_{LHV}$/a** | **1674.8 $TJ_{LHV}$/a** |
| heat extracted from geological reservoir | 838.7 TJ/a | - |
| **$CO_2$ Sequestrated (Removed)** | **207,276.9 t $CO_2$/a** | **0 t $CO_2$/a** |
| Biomass energy utilization factor (Equation (1)): | | |
| gross (annual average) | 43.45% | 48.26% |
| net (annual average) | 37.24% | 47.24% |
| Electrical efficiency (Equation (2)): | | |
| gross (annual average) | 25.97% | 26.09% |
| net (annual average) | 19.76% | 25.07% |
| Gross power to heat ratio of the CHP plant | 0.48 | 1.18 |

* including a biomass-fired CHP plant, $CO_2$ capture and compression installation, and a $CO_2$-enhanced geothermal system with an $sCO_2$ Brayton power cycle.

In Table 6, the presented results indicate that the average biomass energy efficiency (BEUF) is rather low, which is the result of the significant heat demand in the $CO_2$ capture installation. For the BEUF net efficiency, the decrease in comparison with the reference plant for this study is of 10 percentage points. The electrical efficiencies of the analyzed system are also lower than those in the literature (e.g., a 28.2% net annual average in [81] for medium—80 $MW_{ch}$ feed—wood chip CHP with a power-to-heat ratio of 1), but the decrease in the net electricity efficiency in comparison with the reference CHP plant without $CO_2$ capture and utilization in this study is only 5.3 percentage points. It should also be noted that, to keep the same heat and net electrical production, the power-to-heat ratio of the CHP plant changes significantly (from 1.18 in the reference case to 0.48 in the analyzed system), which also strongly affects the technical design of the steam cycle. If geothermal energy would be included in the efficiency calculations, then the net energy utilization factor would be 26.7% and the net electrical efficiency would be 14.2%. The negative $CO_2$ emissions of 97.56 t $CO_2/TJ_{ch}$ are similar to those obtained in the case of CHP plants with a calcium-looping $CO_2$ capture [23].

In Figure 8, the annual electricity balance of the analyzed system is presented. It should be noted that the $sCO_2$ cycle net electricity generation compensates around 73% of the electricity consumption

in the $CO_2$ capture and compression unit. Thus, from the energy point of view, the $CO_2$ utilization in EGS instead of conventional storage in saline formations (which would actually require additional electricity, e.g., for brine management [82]) is more favorable.

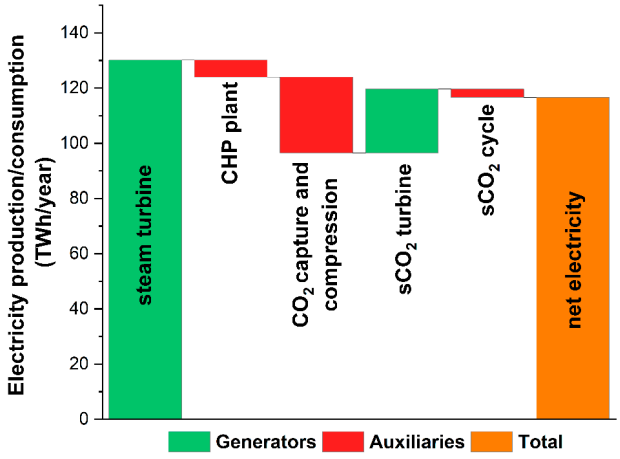


**Figure 8.** Annual electricity balance of the analyzed system.

The SPECCA for the analyzed system, compared to that for the reference CHP plant (biomass-fired without CCS), is 2.17 $MJ_{LHV}$/kg $CO_2$. When the specific energy consumption for $CO_2$ avoided includes the geothermal energy, the value increases significantly to 6.22 MJ/kg $CO_2$. The obtained values of SPECCA, which takes into account only the chemical energy of biomass, can be considered as very low, compared to those for other $CO_2$ capture technologies (e.g., for MEA, the base case is 3.34 $MJ_{LHV}$/kg $CO_2$ in [3]). This is a direct result of the heat integration between the $CO_2$ capture and compression unit and the DHS, as well as the partial compensation of the electricity consumption for $CO_2$ compression in the $sCO_2$ power cycle. The system that excludes the $CO_2$-EGS and assumes conventional $CO_2$ storage, the SPECCA is equal to 3.41 $MJ_{LHV}$/kg $CO_2$, and is comparable with the values from [83] for analyzed $CO_2$ capture technology.

In Figure 9, the energy balance of the analyzed system is presented, showing the main heat losses (cooling duty), the heat load (both for the DHS and MEA regeneration process heat), and electricity production and consumption. As shown, the main cooling duty is associated with the $sCO_2$ cycle, where the excess heat is rejected to the environment. It should be noted that rejected heat in the $sCO_2$ cycle has high parameters (around 110 °C), which means that it could be utilized if possible. It can be also noted that a significant amount of heat is used for MEA regeneration in the $CO_2$ capture unit, which leads to almost a triplication of the overall heat production in the system compared with the reference plant.

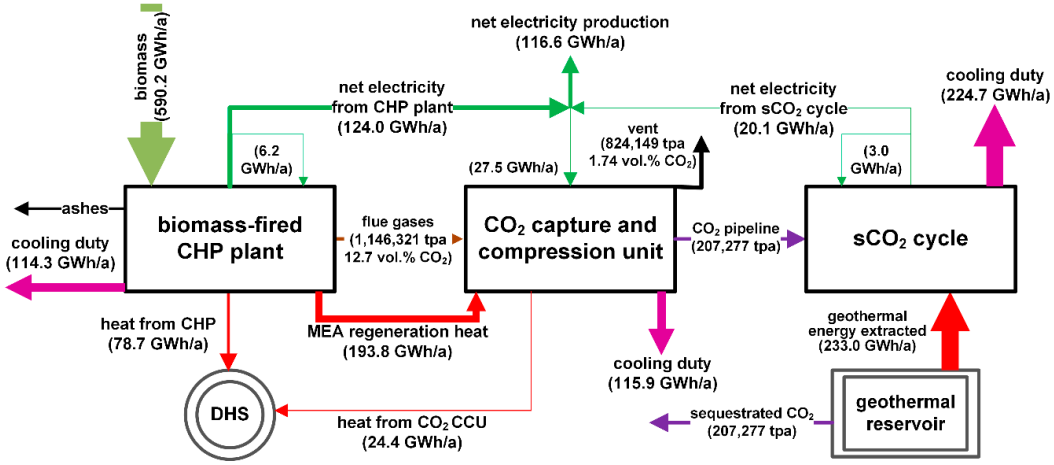


**Figure 9.** Simplified schematic of the analyzed system with the main components of the mass and energy balance.

### 3.2. Economic Evaluation

The TSC of the analyzed system was estimated based on Equation (3) and Appendix B at 153.38 $MEUR_{2017}$. In Figure 10, the share of the TSC for the CHP plant, the $CO_2$ capture and storage unit, the $CO_2$ transport pipeline, the $CO_2$-EGS, and the $sCO_2$ power plant is presented. As can be seen, the cost of the $CO_2$ capture and compression plant is nearly double the investment cost of the plant side. The $CO_2$ transport and utilization (through $CO_2$-EGS and the $sCO_2$ power plant) comprise 20.5% of the TSC, where the development (drilling and fracturing) of the $CO_2$-EGS system is dominant.

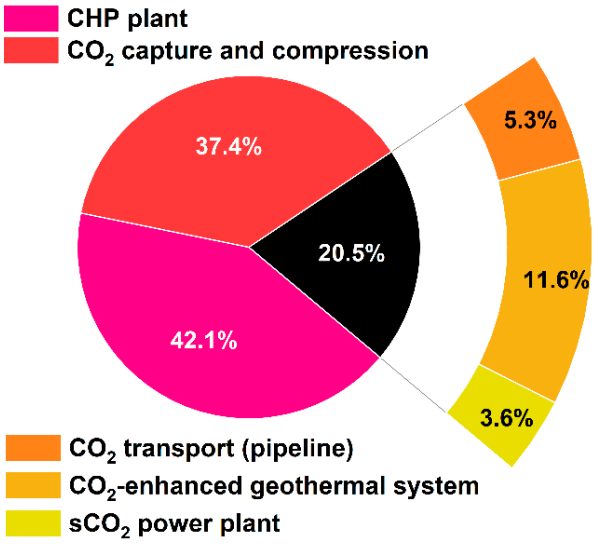


**Figure 10.** The share of system costs for parts of the analyzed system with respect to the total system cost.

The specific unit investment cost was derived from the total subsystem costs, for which the values are as follows:

- The biomass-fired CHP plant: 3073 $EUR/kW_{el}$ (gross electric power in full-condensation mode);
- The MEA unit and the $CO_2$ compression train: 277.5 EUR/tpa;
- The $sCO_2$ power plant and $CO_2$-EGS: 7090 $EUR/kW_{el}$ (gross electric power of the turbine).

In the case of the biomass-fired CHP plant, the values are within the range of medium-size CHP plants fired with wood in the European market, whereas they were 2817 $EUR/kW_{el}$ in the reference case. For the enhanced geothermal plants, the TSC is almost 100% higher [84] compared with the conventional geothermal plants. For the $CO_2$ capture and compression unit, the unit investment costs are also higher (by 30%–50%) when compared with some industrial applications [85], mainly due to the small scale. Nevertheless, the presented results for the cost estimations will be further used in the economic assessment of the whole system, including in technological development scenarios. Within the analysis, three years of construction time is assumed.

For the analyzed system, in the business as usual scenario, the LCOE is equal to 239.0 EUR/MWh and the LCOH is equal to 9.4 EUR/GJ. When the LCOH is still within an acceptable range, the LCOE is significantly higher than it is in other RES schemes [84]. However, it should be noted here that none of the other RES schemes analyzed in [84] have been able to provide negative $CO_2$ emissions, which is one of the main goals of the proposed system. When the reference CHP plant is considered, the LCOE is 127.5 EUR/MWh and the LCOH is 5.0 EUR/GJ. In Table 7, the results of the NPV and BEP for all three analyzed scenarios are presented. In all cases, the NPV is below 0, but what is worth mentioning regarding the subsidy scenario (Figure 11a) is that negative cash flow could be observed—the same comment can be made for the reference CHP plant (Figure 11b). This means that the subsidy for investment cost, without support for operational costs (e.g., through a feed-in tariff for electricity), does not achieve its purpose. As already mentioned, in the current support system in Poland, a feed-in tariff for electricity

and subsidy grants for investment in RES schemes exclude each other to a large degree. In both cases for the analyzed system, the total state subsidy (resulting from a feed-in tariff and investment grants) is around 80 million EUR. As presented in Table 7, in the investment subsidy scenario, the current feed-in tariff of ca. 100 EUR/MWh would need to be increased by 30% to meet the BEP, which would only allow one to obtain NPV = 0 (and this is still not attractive for potential investors).

**Table 7.** Summary of the economic assessment.

| Parameter/Scenario | Business as Usual | Investment Subsidy Scenario | Technological Development |
|---|---|---|---|
| Net Present Value (NPV)—**Analyzed System**, with: | −127,862,030 EUR | −98,362,265 EUR | −66,782,545 EUR |
| Break-Even Point (BEP) for: | | | |
| price of electricity | 243.5 EUR/MWh | 131.6 EUR/MWh | 162.8 EUR/MWh |
| price of heat | 55.1 EUR/GJ | 35.6 EUR/GJ | 29.7 EUR/GJ |
| price of $CO_2$ credits | 100.7 EUR/t $CO_2$ | 65.9 EUR/t $CO_2$ | 55.3 EUR/t $CO_2$ |
| Net Present Value (NPV)—**Reference Biomass-Fired CHP Plant**, with: | −23,751,231 EUR | −45,244,659 EUR | 2,136,259 EUR |
| Break-Even Point (BEP) for: | | | |
| price of electricity | 126.7 EUR/MWh | 86.9 EUR/MWh | 98.00 EUR/MWh |
| price of heat | 18.4 EUR/GJ | 21.6 EUR/GJ | 9.37 EUR/GJ |
| price of fuel | 4.2 EUR/GJ | 3.4 EUR/GJ | 6.1 EUR/GJ |
| **$CO_2$ Avoidance Cost (CAC),** calculated based on Equation (8) | **63.0 EUR/t $CO_2$** | **27.3 EUR/t $CO_2$** | **35.5 EUR/t $CO_2$** |
| $CO_2$ negative emission cost (CNC), calculated based on Equation (9) | 48.2 EUR/t $CO_2$ | 20.9 EUR/t $CO_2$ | 27.1 EUR/t $CO_2$ |

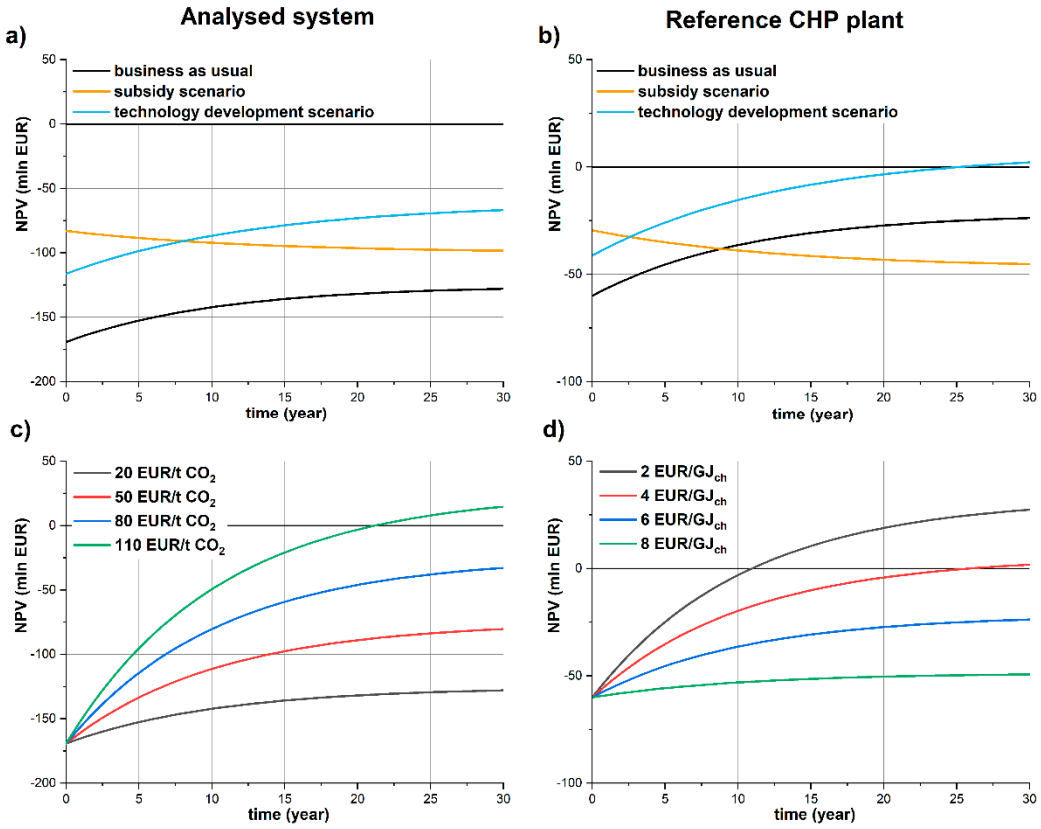


**Figure 11.** The Net Present Value (NPV) for different scenarios in (**a**) the analyzed system and (**b**) the reference biomass-fired CHP plant, and for the business as usual scenario impact of different (**c**) negative $CO_2$ emission credits in the analyzed system and (**d**) prices of fuel in the reference biomass-fired CHP plant.

In Figure 11c, the impact of the negative $CO_2$ emission credit on the NPV for the analyzed system in the business as usual scenario is presented. As there is currently a lack of dedicated schemes to support the negative $CO_2$ emissions, in the analysis, the corresponding EU-ETS $CO_2$ emission allowance price was assumed (20 EUR/t $CO_2$). For the current technological development and economic support mechanism, the price of the negative $CO_2$ emission credits would need to be five times higher to provide economic justification for investment in the analyzed system. For the reference biomass-fired CHP plant, the impact of the fuel cost on the NPV in the same business as usual scenario has been presented in Figure 11d. As can be observed, the cost of fuel significantly impacts the economic profitability of the reference CHP plant, and prices below 4 EUR/$GJ_{ch}$ would be needed to provide economic justification for such units.

In Table 7, beside the NPV for the analyzed system and reference CHP plant, the results for the BEP price of $CO_2$ credits, $CO_2$ avoided cost, and $CO_2$ negative emission cost are presented. Taking into account their definitions, as expected, the BEP of $CO_2$ credit is higher than CAC or CNC, as it refers to the overall economic performance of the analyzed system expressed by the NPV. The CAC is higher than CNC, as it refers to the avoided $CO_2$ emissions, which takes into account the difference in direct $CO_2$ emissions resulting from fuel combustion in the analyzed system and reference plant. Finally, the CNC refers only to obtained negative emissions, which correspond directly to the amount of $CO_2$ capture in the analyzed system, as the reference CHP plant $CO_2$ emission (coming from biomass combustion) is considered to be zero.

As the annual net production of electricity and heat in the analyzed system and reference CHP plant are the same (Table 6), the lowest CAC was obtained for the investment subsidy scenario, in which the investment cost decreases by 50% (through subsidies), followed by the technology development scenario, where the investment cost decreases by 30% (Table 5). Thus, the impact of the investment cost on the CAC can be observed. Taking into account the main goal of the proposed system, which is to obtain negative $CO_2$ emissions, the CNC is a more valuable indicator that quantifies the cost of providing those negative emissions, taking into account the same production levels (in this analysis, electricity and heat) in the energy system. Based on the presented results, it can be stated that the direct cost of negative $CO_2$ emissions coming from the investment in the proposed $CO_2$ capture and utilization (and storage) is around 50 EUR/t $CO_2$, but the economic justification for the development of the analyzed system is two times higher (around 100 EUR/t $CO_2$) in the business as usual scenario.

In Figure 12, the discounted cash flow (CF) for the analyzed system is presented. It can be observed that incomes from electricity and heat barely surpass the operational expenditures (fixed and variable operational costs). Thus, the NPV values (e.g., for the business as usual scenario) correspond to the TSC.

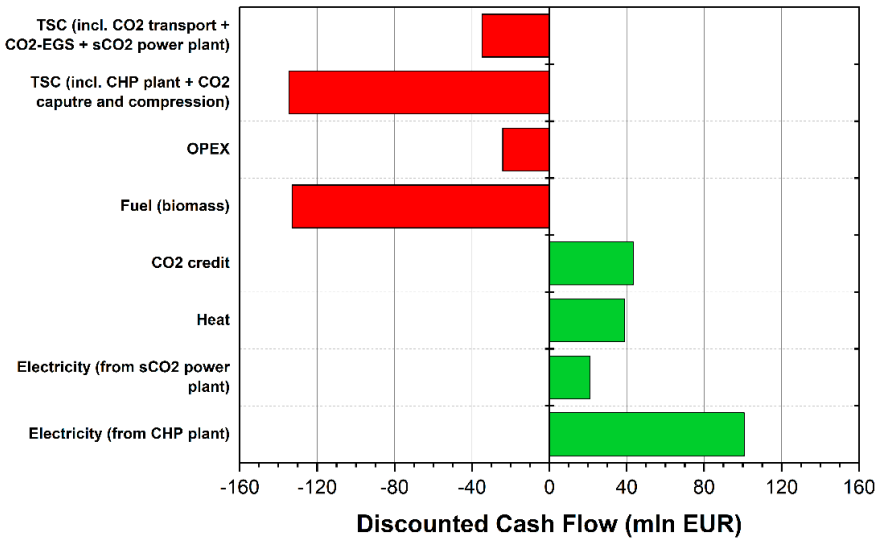


**Figure 12.** Discounted CF in the business as usual scenario in the analyzed system.

For the performed economic assessment, sensitivity analysis was performed, and the results are presented in Figure 13. As expected, the price of electricity and fuel (biomass) has the highest impact on the NPV. The impact of the price of heat and price of negative $CO_2$ emission credit has a similar effect, although it should be pointed out that the heat price is strictly regulated in Poland, so significant changes in the price of heat should not be expected. Moreover, a dedicated support scheme for heat production operational costs from renewable energy sources is also lacking.

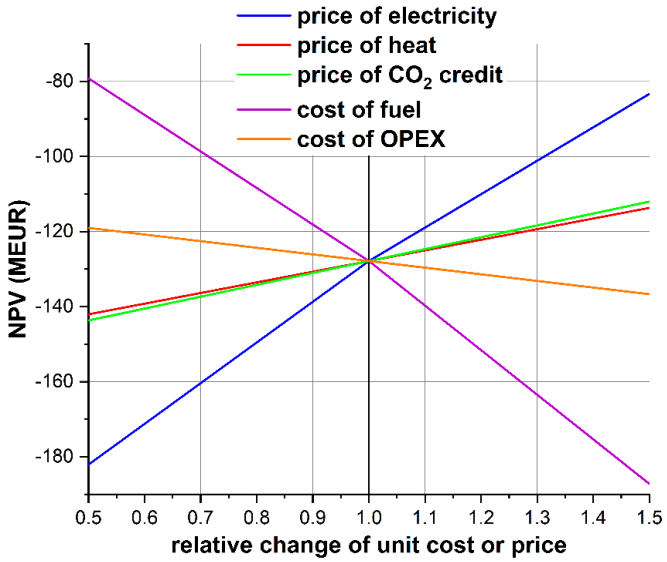


**Figure 13.** Sensitivity analysis in the business as usual scenario in the analyzed system.

In Figure 14, the NPV in the function of the cost of fuel and the price of negative $CO_2$ emission credit is presented for the business as usual and the technological development scenarios. It is clear that, with an increase of the price of biomass (fuel), a lower NPV can be obtained. On the other hand, the increase in the $CO_2$ credits helps to increase the profitability of the project. With a decrease in the costs of fuel to 4 EUR/GJ (which is a closer price range in, e.g., the USA) and the technological development of the system components (which is possible, taking into account, e.g., the decrease in the investment cost for other renewable energy source technologies and $CO_2$ capture technology itself), the BEP of the negative $CO_2$ emission credit is around 35 EUR/t $CO_2$, which is a very promising option for heat and electricity supply together with carbon dioxide removal from the atmosphere.

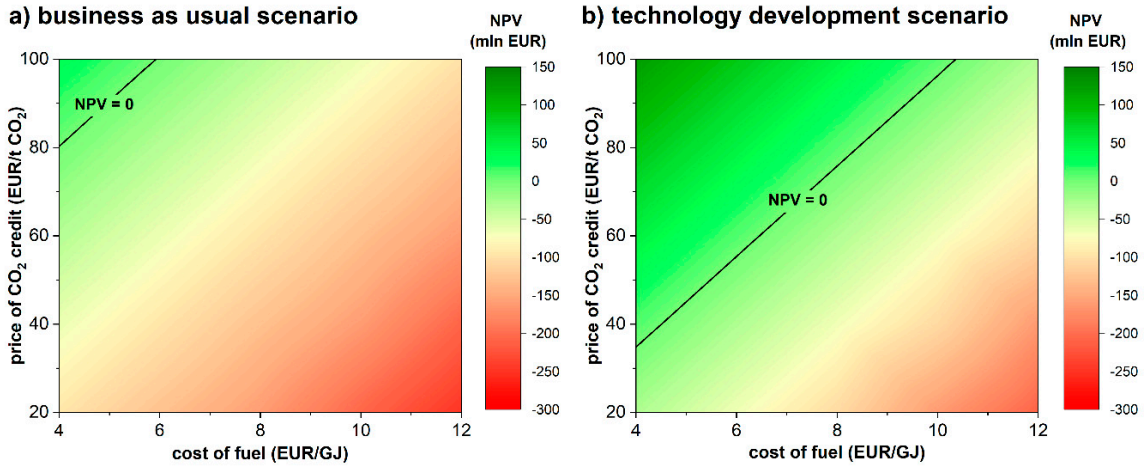


**Figure 14.** NPV in the function of negative $CO_2$ emission credits and the cost of fuel in (**a**) the business as usual scenario and (**b**) the technological development scenario.

Within the analyzed system, the TSC includes the costs associated with $CO_2$ utilization—the $CO_2$ transport pipeline, $CO_2$-EGS system development (drilling and fracturing), and the $sCO_2$ power plant. This approach might not correspond to current trends in CCUS technologies, while dedicated operators are proposed for $CO_2$ transport and $CO_2$ utilization or storage.

In Figure 15, the impact including the proposed CCUS chain associated with $CO_2$ transport and utilization on the NPV is presented. The black lines correspond to the currently analyzed option for two $CO_2$ transport distances (50 and 100 km). The coloured lines indicate the impact on the NPV when the costs of $CO_2$ transport and storage (T&S) are given. As can be seen, the proposed option (for a 50 km $CO_2$ transport pipeline) is competitive when the $CO_2$ transport and storage costs are above 10 EUR/t $CO_2$ (which is the case for Poland [82]). This proves that the proposed design of $CO_2$ transport and utilization (including storage) is an economically favorable option, and that the electricity production from renewable energy sources (geothermal energy) can be increased.

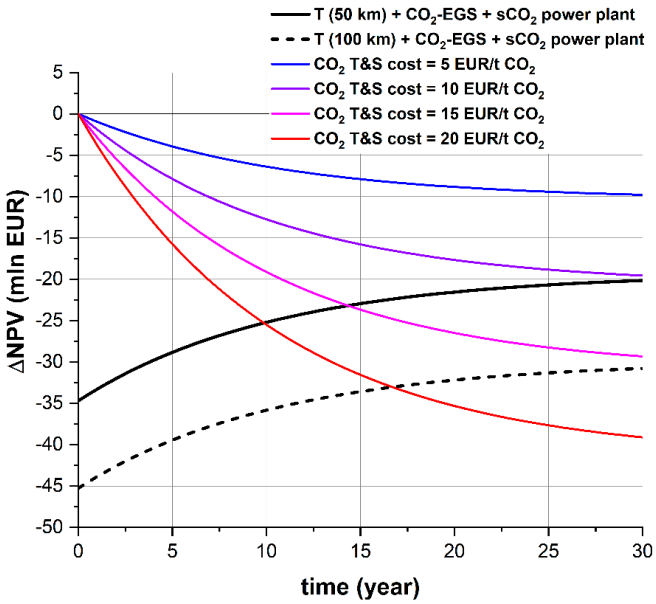


**Figure 15.** ΔNPV resulting from different options for capture $CO_2$ utilization and storage.

### *3.3. Technology Readiness Level of the Analyzed Concept*

The concept of the Technology Readiness Level (TRL) is used to estimate the maturity level of a technology, which is necessary to achieve a low-carbon economy but not yet available at a commercial scale. One of them is CCS, including BECCS. However, there are factors that can put important limitations on its global spread. These include a lower efficiency compared to other combustion methods and a weak infrastructure for $CO_2$ transport and storage. On the combustion side, a lower energy density and less ash deposition can be problematic [86]. However, the key prerequisites for large-scale BECCS are the availability of biomass feedstock and land for production. The challenges for the former include competition between different sectors of the economy for feedstock and competition with other ecosystem services, for example food production. The seasonal availability of certain crops can also be a limitation. A related issue is land availability for biomass feedstock production. BECCS is one of the CCS technologies that have reached (or are close to reaching) the commercial phase of development. What is underlined by researchers is that BECCS' spread relies on a mature CCS industry. In 2019, five BECCS plants were operating worldwide. By 2100, this could provide more than 5% of total global primary energy [87]. However, if other negative emission technologies are to be quickly developed, this could potentially lead to a slower and lower uptake of BECCS. This can only be realized if they are to be cost-competitive in comparison to BECCS [87].

There were four EGS sites in the US in 2017, operating at around a 2 $MW_{el}$ capacity. Some of them are planned to reach 5 $MW_{el}$ by 2020. However, the small project size can be misleading, as *the target is the development of (low- and medium-temperature) geothermal systems in the range of hundreds of kWe to an MWe for electricity in remote towns as well as the utilization of coproduced thermal power generation that results from the by-products of existing oil and gas wells.* Only afterwards is the development of larger systems planned [42]. There have been attempts to develop an EGS in Asia as well. Japan developed two, but they are now closed. South Korea, China, and Taiwan are currently experimenting with the technology [42,88]. It has also been recently argued that, despite promising initial ideas on applying unconventional oil and gas technologies, there are shortcomings that make EGSs uneconomical [89]. Research has indicated that an adequate mass flow rate, of 80 kg/s at 200 °C, is required for the proper functioning of an EGS plant. However, the systems currently in operation do not even reach 25 kg/s [90]. Moreover, the costs of deep wells remain highly uncertain [90]. The key challenge that remains addressed is how to establish and maintain a suitable reservoir. Furthermore, its change over time is insufficiently understood. Finally, knowledge on the long-term interaction between working fluids and rock structure is incomplete [91]. To sum up, EGSs are heavily subsidized and are more expensive than other energy sources, which makes them not economically feasible. Therefore, governments should focus on reducing costs to 2030 to a competitive level [88]. This is assuming remarks that refer to a water-based EGS, while the TRL level of a $CO_2$-based EGS is around 3–4.

There are five research institutes in the US and one each in Japan and South Korea that have indicated experimentation with $sCO_2$ since 2009 [48,92]. According to the energetic rule of thumb that thermal efficiency rises with the size of the system, $sCO_2$ efficiency is expected to rise. However, all test facilities operate at small scales; therefore, the development of a large-scale (>10 MW) prototype $sCO_2$ system is necessary [92], and some of the most recent research points out that scaling up remains an issue [47,48]. Better designs of heat exchangers, bearings, and seals are necessary [47]. Two experiments of the application of the $sCO_2$ power cycle in geothermal energy have shown that (1) the relationship between the mass flow rate of $sCO_2$ and the power capacity is nonlinear and that (2) the cycle efficiency was around 18% [47]. Thus, the overall TRL is also rather low, around 4–5.

Thus, taking into account all of the aforementioned considerations, the overall TRL of the proposed concept can be assessed as TRL4 (technological development), mainly due to the early stage of the $CO_2$-enhanced geothermal system development.

## 4. Discussion

Based on the presented results, it can be concluded that, in the current energy market in Poland, the proposed option is not economically feasible. The break-even price of the negative $CO_2$ emission credit (the $CO_2$ emission allowance price) should be approximately 100 EUR/t $CO_2$, which, even with the latest rapid increase in EU ETS prices, could be expected by 2050. Within the analyzed scenarios, the government investment subsidies could improve the economic profitability of the system, but this is still not enough to provide economic justification at present without further support for the operational costs (e.g., through a feed-in tariff for electricity or additional negative $CO_2$ emission credits). Thus, further technological advances should be pursued to lower the investment costs of system components, mainly of the CHP plant, post-combustion $CO_2$ capture, and $CO_2$-EGS system development (the cost of wells drilling). In the first case, the potential is already visible when comparing the investment costs around the world—e.g., in China and India, the unit investment costs for biomass-fired CHP plants are almost two times lower than in Europe [84]. Additionally, a decrease in the $CO_2$ capture installation investment cost should also be expected due to the development and maturity, as well as the redesign, of the units for smaller capacities. In addition, there is still small room for improved energy performance, as a decrease in the energy consumption in $CO_2$ capture units can be observed.

Where operational costs are concerned, fuel cost is of great significance; the assumed paper price of 6 EUR/GJ for waste wood biomass in Poland seems higher than in other parts of the world—e.g., in the USA, the prices are up to 2.5 USD/GJ [93]—but if the transport to Europe and other costs are

included, in the end, the prices of biomass are even higher (up to 10 USD/GJ). The prices of wood biomass are expected to grow over the next several years in Poland, so only a locally specific source of cheap biomass could positively influence the economic profitability of the system.

From an economic point of view, $CO_2$ utilization instead of conventional storage in saline formations proved to be more economically justified, as the sequestration during the operation of the $CO_2$-EGS system could generate additional income per unit of $CO_2$ stored. The low electrical efficiency of the $CO_2$-EGS power plant can be significantly improved when additional ORC is added or there is a local demand for heat at the site. Those options should be analyzed in further studies to estimate the potential economic benefits resulting from the change in system design.

In [94], the cost of BECCS was estimated between 15 and 400 USD/ton of $CO_2$ removed. It was also stated that BECCS was the best solution for providing negative $CO_2$ emissions in most climate change scenarios. It should be noted that BECCS also has several drawbacks—mainly increased water and land use [94].

Where the maturity of the analyzed technological design is concerned, the conventional BECCS components are usually mature technologies. In the analyzed system, the $CO_2$-EGS system was included, which would decrease the TRL of the technology. However, as stated in the introduction, Poland still has much to do in the field of regulations and laws for CCS deployment, and probably even more where CCUS is concerned. Nevertheless, despite rather negative results coming from the study, research should be continued in terms of whole system energy and economic optimization, as well as more detailed investment cost estimations. Taking into account the importance of negative $CO_2$ emissions for meeting climate goals [10], there might not be a better alternative than the wide deployment of BECCS technologies.

## 5. Conclusions

The obtained results indicate that, in the current energy market in Poland, the proposed system is not economically feasible. The main obstacles, from an economic point of view, are associated with the high investment cost of the $CO_2$ capture and compression unit, as well as a lack of dedicated comprehensive governmental incentives to pursue negative $CO_2$ emissions in the energy sector. The latter is associated with the general lack of interest on behalf of the Polish government in $CO_2$ capture and storage technologies, despite their general increased technological maturity over the last few years.

**Author Contributions:** Conceptualization, P.G.; methodology, P.G. and M.M.; software, P.G. and M.M.; validation, P.G., A.S. and M.M.; formal analysis, P.G. and M.M.; investigation, P.G., M.M. and M.H.; resources, P.G., A.S. and L.P.; data curation, P.G., M.M. and A.S.; writing—original draft preparation, P.G., A.S., M.M., L.P. and M.H.; writing—review & editing, P.G., A.S., M.M. and M.H.; visualization, P.G. and A.S.; supervision, P.G.; project administration, P.G.; funding acquisition, P.G. All authors have read and agreed to the published version of the manuscript.

**Funding:** This research was funded by the National Science Centre, Poland, grant number 2017/24/C/ST8/00204.

**Conflicts of Interest:** The authors declare that there is no conflict of interest.

## Appendix A

Governing equations for steady-state, single-channel flow and heat exchange in the reservoir–wellbore coupled model are presented in Appendix A. From the law of energy conservation and assuming a Darcy flow of constant cross-sectional area in the reservoir, the following set of equations is used to estimate the necessary injection pressure to be maintained at the wellhead:

$$P_{inj} = P_{res} + \Delta P_{f,\,well} + \Delta P_{res} - \rho g \Delta z \tag{A1}$$

$$\Delta P_{f,\,well} = f\frac{\Delta z}{D}\rho\frac{V^2}{2} = 8f\frac{\Delta z \dot{m}^2}{\pi^2 \rho D^5} \tag{A2}$$

$$f = \left[-1.8 \log\left(\frac{6.9}{Re} + \left(\frac{\xi}{3.7D}\right)\right)\right]^{-2} \tag{A3}$$

$$Re = \frac{\rho V D}{\mu} = \frac{4\,\dot{m}}{\mu \pi D} \tag{A4}$$

$$\Delta P_{res} = \frac{\dot{m}\,\mu \Delta L}{\rho K A} \tag{A5}$$

For the production well, the following relationship is valid:

$$P_{prod} = P_{res} - \Delta P_{f,\,well} - \rho g \Delta z \tag{A6}$$

where $P_{inj}$ and $P_{prod}$ are the pressures at the wellheads of the injection and production wells, respectively; $\Delta P_{f,\,well}$ represents the frictional pressure loses in the wellbore; $\Delta P_{res}$ represents the reservoir pressure losses due to laminar (Darcy) flow; V is the fluid velocity; $\dot{m}$ is the mass flow rate; $\rho$ is the fluid density; $\mu$ is the fluid dynamic viscosity; Re is the Reynolds number; g is the standard gravity; D is the pipe inner diameter; $\xi$ is the pipe roughness; K is the average permeability of the reservoir zone; $\Delta L$ and $\Delta z$ are the incremental reservoir and well intervals (lengths), respectively; and A is the cross-sectional swept area of the fluid flow in the reservoir.

The temperature of the working fluid (e.g., water and $CO_2$) at the bottom of the injection well and at the production wellhead can be estimated using the approximate solution of the line-source heat equation. The solution of Equation (A7) allows for the determination of the unit heat transfer rate between the borehole and flowing well.

$$q_I = 4\pi\lambda_a (T_w - T_\infty)\left[\ln\left(\frac{4\lambda_z t}{r_w^2 c_r \rho_r}\right) - \gamma\right]^{-1} \tag{A7}$$

where $q_I$ is the unit heat transfer rate; $\lambda_a$ is the apparent thermal conductivity of the wellbore, casings, and surrounding rock formation; $c_r$ is the specific heat of rock formation; $\rho_r$ is the density of the rock formation; $T_w$ is the temperature of the fluid in the analyzed interval; $T_\infty$ is the natural temperature of the rock formation in the analyzed interval, undisturbed by the drilling of the fluid flow; t is the time; $r_w$ is the well diameter; and $\gamma$ is the Euler constant ($\gamma \approx 0.577216$).

Equation (A7) is valid only when

$$u = \frac{r_w^2 c_r \rho_r}{4\lambda_a t} \ll 1 \tag{A8}$$

The determination of the unit heat transfer rate requires the use of an apparent thermal conductivity coefficient, which takes into account the thermal conductivity of the casings, grouts, and rock formation, at a distance from the well axis to the distance at which the impact of the well operation on the natural temperature of the rock formation is negligible. The apparent thermal conductivity coefficient for cylindrical layers can be determined using Equation (A9):

$$\lambda_a = \frac{\sum_{i=1}^{n} s_i}{\sum_{i=1}^{n} \frac{s_i}{\lambda_i} \frac{D_{mz}}{D_{mi}}} \tag{A9}$$

where $s_i$ is the thickness of the ith layer, $\lambda_i$ is the thermal conductivity of the ith layer, $D_{mz}$ is the equivalent logarithmic mean of the extreme diameters, and $D_{mi}$ is the logarithmic mean of the outer and inner diameters of the ith cylindrical layer (m).

$$D_{mz} = 4\sqrt{\alpha t} \tag{A10}$$

where $\alpha$ is the thermal diffusivity of rock formation, and t is the time of the simulation period (1 year).

The formula for the logarithmic mean of the pipe diameters is

$$D_m = \frac{D_{out} - D_{inn}}{\ln \frac{D_{out}}{D_{inn}}} \quad (A11)$$

where $D_{out}$ and $D_{inn}$ are the pipe's outer and inner diameters, respectively.

The temperature at the outlet of each borehole's interval can be calculated using the following equation:

$$T_{out,\,i} = T_{inn,\,i} - \frac{q_{I,i}\, z_i}{\dot{V}\, c\rho} \quad (A12)$$

where $T_{out,\,i}$ and $T_{inn,\,i}$ are the temperatures at the outlet and inlet of the ith section, respectively; $l_i$ is the length of the ith section; $\dot{V}$ is the volumetric flow rate; c is the specific heat; and $\varrho$ is the density of the injected/pumped fluid (kg/m$^3$).

## Appendix B

All total equipment cost (TEC) values are given in EUR (2017). The TECs were given as "power functions" for the following components:

- The biomass receiving and preparation infrastructure:

$$TEC_{RPI} = 332,786 \times \dot{G}_{bio}^{0.4096} \quad (A13)$$

where $\dot{G}_{bio}$ (ton/day) is the biomass mass flow (as received);

- The biomass grate boiler:

$$TEC_{GB} = \dot{m}_{st} \times \left(274\,352 \times \dot{m}_{st}^{-0.1195}\right) \times C_{p,GB} \times C_{t,GB} \quad (A14)$$

where $C_{p,GB}$ and $C_{t,GB}$ stand for the pressure and superheated steam multipliers:

$$\begin{cases} C_{p,GB} = 1 & p_{st} \le 2.0\,MPa \\ C_{p,GB} = -0.0278 \times p_{st}^2 + 0.5348 \times p_{st} + 0.0044 & \text{for} \quad 2.0\,MPa < P_{st} < 6.0\,MPa \\ C_{p,GB} = 2.21 & P_{st} \ge 6.0\,Mpa \end{cases} \quad (A15)$$

$$C_{T,GB} = -0.9 \cdot 10^{-6} \times \Delta T_{st}^2 + 0.0043 \times \Delta T_{st} + 1.0051 \quad (A16)$$

where and $\dot{m}_{st}$ (kg/s) is the boiler steam mass flow, $p_{st}$ (MPa) is the boiler steam pressure, and $\Delta T_{st}$ (K) is the difference between the steam temperature from the boiler and saturation temperature;

- The extraction-condensing steam turbine:

$$TEC_{EC,ST} = \left(4008.22 \times P_{ST,con}^{-0.287}\right) \times P_{ST,con} \quad (A17)$$

where $P_{ST,con}$ ($kW_{el}$) is the electrical power of the turbine in full-condensation mode;

- The water/steam heat exchangers:

$$TEC_{WS,HX} = \left(313 \times \dot{Q}_{HX}^{-0.18}\right) \times \dot{Q}_{HX} \quad (A18)$$

where $\dot{Q}_{HX}$ ($kW_{th}$) is the heat transfer in the heat exchanger;

- The air fans:

$$TEC_{AF} = 103,193 \times \left(\frac{P_{AF}}{445}\right)^{0.67} \tag{A19}$$

where $P_{AF}$ ($kW_{el}$) is the electrical power of the air fan motor;

- The electrical generator:

$$TEC_{GEN} = 85.4 \times P_{GEN}^{0.95} \tag{A20}$$

where $P_{GEN}$ ($kW_{el}$) is the electrical power of the generator;

- The cooling tower:

$$TEC_{CT} = 32.2 \times \dot{Q}_{CT} \tag{A21}$$

where $\dot{Q}_{CT}$ ($kW_{th}$) is the cooling tower heat duty;

- The supercritical $CO_2$ turbine:

$$TEC_{CO2,ST} = 168,840 \times P_{ST}^{0.8} \times C_{p,CO2} \times C_{t,CO2} \tag{A22}$$

where $P_{ST}$ ($MW_{el}$) is the effective power of the turbine, and $C_{p,CO2}$ and $C_{t,CO2}$ stand for the pressure and temperature multipliers for the $sCO_2$ machinery:

$$\begin{cases} C_{p,CO2} = 1 \text{ if } p_{max} < 10\ MPa \\ C_{p,CO2} = 0.8 + 0.02 \times p_{max} \text{ if } p_{max} \geq 10\ MPa \end{cases} \tag{A23}$$

$$\begin{cases} C_{t,CO2} = 1 \text{ if } t_{max} < 400 \\ C_{t,CO2} = 5.32 - 0.0238 \times t_{max} + 0.00003 \times t_{max}^2 \text{ if } t_{max} \geq 400 \end{cases} \tag{A24}$$

where and $p_{max}$ (bar) is the maximal pressure, and $t_{max}$ (°C) is the maximal temperature at which the machinery is operated;

- The supercritical $CO_2$ chiller:

$$TEC_{CO2,HX} = 168 \times UA_{HX} \times C_{p,CO2} \times C_{t,CO2} \tag{A25}$$

where $UA_{HX}$ (kW/K) is the overall heat transfer coefficient U multiplied by the heat transfer area A of the heat exchanger.

For the $CO_2$ capture and compression equipment, the total equipment cost was estimated as

$$TEC = TEC_{ref} \times \left(\frac{X}{X_{ref}}\right)^{0.6} \tag{A26}$$

where X is the scaling parameter. For the components of the $CO_2$ capture and compression equipment, the scaling parameters are presented in Table A1.

**Table A1.** Scaling parameters for the $CO_2$ capture and compression equipment.

| Equipment | Scaling Parameter, $X$ |
|---|---|
| Direct contact cooler<br>Flue gas blower<br>Absorber | $\frac{\dot{V}_{fg}}{\dot{V}_{fg,ref}} \times \frac{T_{fg}}{T_{fg,ref}}$ |
| Rich/lean cross heat exchanger<br>Regenerator | $\frac{\dot{V}_{solv}}{\dot{V}_{solv,ref}}$ |
| Reboiler | $\frac{\dot{V}_{fg}}{\dot{V}_{fg,ref}} \times \frac{\dot{G}_{st}}{\dot{G}_{st,ref}}$ |
| Steam extractor | $\frac{\dot{G}_{st}}{\dot{G}_{st,ref}}$ |
| MEA reclaimer | $\frac{\dot{G}_{\Delta MEA}}{\dot{G}_{\Delta MEA,ref}}$ |
| Solvent processing area | $\frac{\dot{V}_{solv}}{\dot{V}_{solv,ref}}$ |
| $CO_2$ drying and compression unit | $\frac{\dot{G}_{CO2}}{\dot{G}_{CO2,ref}}$ |

where $\dot{V}_{fg}$ is the flue gas volumetric flow; $T_{fg}$ is the flue gas temperature at the inlet to given machinery; $\dot{V}_{solv}$ is the solvent volumetric flow; $\dot{G}_{st}$ is the steam mass flow; $\dot{G}_{\Delta MEA}$ is the make-up solvent mass flow; and $\dot{G}_{CO2}$ is the compressed $CO_2$ mass flow.

For the $CO_2$ transport pipeline, the following formula was used to estimate the total system cost:

$$TSC_{pipeline} = \left[\left(9745.6 \times \dot{G}_{CO2}^{0.35}\right) \times L_{pipeline}^{0.13}\right] \times L_{pipeline} \quad \text{(A27)}$$

where $\dot{G}_{CO2}$ (ton/day) is the $CO_2$ mass flow rate, and $L_{pipeline}$ (km) is the pipeline length.

For the enhanced geothermal system development, including drilling and fracturing, the following formula was used to estimate the total system cost:

$$TSC_{EGS} = (n \times D_{well} \times 1400) + 2,123,800 \quad \text{(A28)}$$

where $n$ is the number of wells, and $D_{well}$ (m) is the depth of the well. Factor 1400 corresponds to the unit drilling cost for wells above 5000 m.

## References


1. Polish Ministry of Economy. *Polish Energy Policy until 2030*; Polish Ministry of Economy: Warsaw, Poland, 2009.
2. Polish Ministry of Development. *Responsible Development Strategy*; Polish Ministry of Development: Warsaw, Poland, 2017.
3. Global CCS Institute. The Global Status of CCS: 2019. Australia, 2019. Available online: https://www.globalccsinstitute.com/resources/global-status-report/ (accessed on 6 January 2020).
4. Havercroft, I.; Consoli, C. *The Carbon Capture and Storage Readiness Index 2018: Is the World Ready for Carbon Capture and Storage*; Global CCS Institute: Melbourne, Australia, 2018.
5. Global Carbon Atlas. Available online: http://www.globalcarbonatlas.org/en/content/welcome-carbon-atlas (accessed on 6 January 2020).
6. Consoli, C. *CCS Storage Indicator (CCS-SI)*; Global CCS Institute: Melbourne, Australia, 2018.
7. Havercroft, I.; Consoli, C.; Zapantis, A. *Carbon Capture and Storage Policy Indicator (CCS-PI)*; Global CCS Institute: Melbourne, Australia, 2018.
8. Havercroft, I. *CCS Legal and Regulatory Indicator (CCS-LRI)*; Global CCS Institute: Melbourne, Australia, 2018.
9. Townsend, A.; Gillespie, A. *Scaling up the CCS Market to Deliver Net-Zero Emissions*; Global CCS Institute: Melbourne, Australia, 2020.

10. The Intergovernmental Panel on Climate Change. Global Warming of 1.5 °C—An IPCC Special Report. Switzerland, 2018. Available online: https://www.ipcc.ch/sr15/ (accessed on 6 January 2020).
11. Minx, J.C.; Fuss, S.; Nemet, G. Guest Post: Seven Key Things to Know About 'Negative Emissions'. CarbonBrief 2018. Available online: https://www.carbonbrief.org/guest-post-seven-key-things-to-know-about-negative-emissions (accessed on 9 January 2019).
12. Karlsson, H.; Byström, L. *Global Status of BECCS Projects 2010*; Global CCS Institute: Canberra, Australia; Biorecro AB: Stockholm, Sweden, 2011.
13. International Energy Agency (IEA) GHG Programme. *Potential for Biomass and Carbon Dioxide Capture and Storage, 20116/06*; International Energy Agency: Cheltenham, UK, 2011.
14. Mika-Bryska, M.; Wróblewska, E. Polskie podejście do CCS w świetle aktualnego statusu rozwoju tej technologii. *Prz. Geol.* **2015**, *63*, 30–33.
15. Skowroński, P. Budowa Instalacji Demonstracyjnej CCS Zintegrowana z Nowym Blokiem 858 MW w Elektrowni Bełchatów. Available online: https://stowarzyszenie-zmijewski.pl/sites/default/files/materialy/skowronski_pawel_pge.pdf (accessed on 9 January 2020).
16. Wróblewska, E. CCS—Polish Point of view. In Proceedings of the BARSREC Conference, Warsaw, Poland, 29 October 2015; Available online: http://basrec.net/wp-content/uploads/2015/11/A-6-Elzbieta-Wroblevska-CCS-Polish-point-of-view.pdf (accessed on 19 October 2019).
17. Urych, T.; Chećko, J.; Stańczyk, K. CCUS in region which is traditionally associated with coal mining and heavy industry. In Proceedings of the CO2GeoNet and Central Mining Institute Event, Katowice, Poland, 10 December 2018; Available online: http://cop24.CO2geonet.com/media/10126/4_ccus-in-region-which-is-traditionally-associated-with-coal-mining-and-heavy-industry.pdf (accessed on 9 January 2020).
18. Polish Ministry of Energy. Ocena Skutków Planowanych Polityk I Środków. Załącznik 2. Do Krajowego Planu na Rzecz Energii I Klimatu Na Lata 2021–2030. Available online: https://www.gov.pl/documents/33372/436746/Za%C5%822_projekt_KPEiK_scenariusz_PEK_2019-01-04.pdf/3ce489ab-d61f-fd61-a42d-559072e5f4ab (accessed on 19 October 2019).
19. Gambhir, A.; Butnar, I.; Li, P.-H.; Smith, P.; Strachan, N. A review of criticisms of integrated assessment models and proposed approaches to address these, through the lens of BECCS. *Energies* **2019**, *12*, 1747. [CrossRef]
20. Stavrakas, V.; Spyridaki, N.-A.; Flamos, A. Striving towards the deployment of bio-energy with carbon capture and storage (BECCS): A review of research priorities and assessment needs. *Sustainability* **2018**, *10*, 2206. [CrossRef]
21. Restrepo-Valencia, S.; Walter, A. Techno-economic assessment of bio-energy with carbon capture and storage systems in a typical sugarcane mill in Brazil. *Energies* **2019**, *12*, 1129. [CrossRef]
22. Keller, M.; Kaibe, K.; Hatano, H.; Otomo, J. Techno-economic evaluation of BECCS via chemical looping combustion of Japanese woody biomass. *Int. J. Greenh. Gas Control* **2019**, *83*, 69–82. [CrossRef]
23. Gładysz, P.; Tynjälä, T.; Hyppänen, T. Biomass-fired combined heat and power plant with calcium looping $CO_2$ capture—Process configuration analysis. In Proceedings of the 5th International Conference on Contemporary Problems of Thermal Engineering, Gliwice, Poland, 18–21 September 2018.
24. Buńczyk, A.; Bogusławski, P. *Energetyka Cieplna w Liczbach—2017*; Energy Regulatory Office: Warsaw, Poland, 2018.
25. Rączka, J.; Rubczyński, A. *The Last Bell for District Heating in Poland*; Regulatory Assistance Project & Forum Energii: Warsaw, Poland, 2017.
26. Rączka, J. *Heating Transformation 2030. Small District Heating System*; Regulatory Assistance Project & Forum Energii: Warsaw, Poland, 2017.
27. Regulski, B. *Przyszłość Ciepłownictwa Systemowego w Polsce (The Future of Heating Sector in Poland)*; Izba Gospodarcza Ciepłownictwo Polskie: Olsztyn, Poland, 2016.
28. Rubczyński, A. *Clean Heat 2030—Strategy for Heating*; Forum Energii: Warsaw, Poland, 2019.
29. Raos, S.; Ilak, P.; Rajšl, I.; Bilić, T.; Trullenque, G. Multiple-criteria decision-making for assessing the enhanced geothermal systems. *Energies* **2019**, *12*, 1597. [CrossRef]
30. Li, M.; Lior, N. Comparative analysis of power plant options for enhanced geothermal systems (EGS). *Energies* **2014**, *7*, 8427–8445. [CrossRef]
31. Tester, J.W.; Anderson, B.J.; Batchelor, A.S.; Blackwell, D.D.; Dipippo, R.; Drake, E.M.; Garnish, J.; Livesay, B.; Moore, M.C.; Nichols, K.; et al. *The Future of Geothermal Energy Impact of Enhanced Geothermal Systems (EGS) on the United States in the 21st Century. An Assessment by an MIT-Led Interdisciplinary Panel*; Massachusetts Institute of Technology: Cambridge, MA, USA, 2006.

32. Aminu, M.D.; Nabavi, S.A.; Rochelle, C.A.; Manovic, V. A review of developments in carbon dioxide storage. *Appl. Energy* **2017**, *208*, 1389–1419. [CrossRef]
33. Cui, G.; Ren, S.; Rui, Z.; Ezekiel, J.; Zhang, L.; Wang, H. The influence of complicated fluid-rock interactions on the geothermal exploitation in the $CO_2$ plume geothermal system. *Appl. Energy* **2018**, *227*, 49–63. [CrossRef]
34. Pruess, K. Enhanced geothermal systems (EGS) using CO2 as working fluid—A novel approach for generating renewable energy with simultaneous sequestration of carbon. *Geothermics* **2006**, *35*, 351–367. [CrossRef]
35. Olasolo, P.; Juárez, M.C.; Morales, M.P.; Olasolo, A.; Agius, M.R. Analysis of working fluids applicable in Enhanced Geothermal Systems: Nitrous oxide as an alternative working fluid. *Energy* **2018**, *157*, 150–161. [CrossRef]
36. Wang, C.L.; Cheng, W.L.; Nian, Y.L.; Yang, L.; Han, B.B.; Liu, M.H. Simulation of heat extraction from $CO_2$-based enhanced geothermal systems considering $CO_2$ sequestration. *Energy* **2018**, *142*, 157–167. [CrossRef]
37. Guo, F.T.; Gong, F.; Wang, X.; Lina, Q.; Qua, Z.; Zhang, W. Performance of enhanced geothermal system (EGS) in fractured geothermal reservoirs with $CO_2$ as working fluid. *Appl. Therm. Eng.* **2019**, *152*, 215–230. [CrossRef]
38. Brown, D.W. A hot day rock geothermal energy concept utilizing super-critical $CO_2$ instead of water. In Proceedings of the Twenty-Fifth Workshop on Geothermal Reservoir Engineering, Stanford, CA, USA, 24–26 January 2000; Available online: https://pangea.stanford.edu/ERE/pdf/IGAstandard/SGW/2000/Brown.pdf (accessed on 6 January 2020).
39. Pritchett, J.W. On the relative effectiveness of $H_2O$ and $CO_2$ as reservoir working fluids for EGS heat mining. *Geotherm. Resour. Counc. Trans.* **2009**, *33*, 235–239.
40. Pruess, K. Enhanced geothermal systems (EGS): Comparing water and $CO_2$ as heat transmission fluids. In Proceedings of the New Zealand Geothermal Workshop, Auckland, New Zealand, 19–21 November 2007.
41. Pruess, K. On production behavior of enhanced geothermal systems with $CO_2$ as working fluid. *Energy Convers. Manag.* **2008**, *49*, 1446–1454. [CrossRef]
42. Lu, S.M. A global review of enhanced geothermal system (EGS). *Renew. Sustain. Energy Rev.* **2018**, *81*, 2902–2921. [CrossRef]
43. Biagi, J.; Agarwal, R.; Zhang, Z. Simulation and optimization of enhanced geothermal systems using $CO_2$ as a working fluid. *Energy* **2015**, *86*, 627–637. [CrossRef]
44. Song, Y.; Wu, X.; Hu, S.; Wang, W. Numerical simulation of heat transfer and sequestration of $CO_2$ hot-dry-rock. *J. Eng. Thermophys.* **2013**, *34*, 1902–1905.
45. Zhang, F.Z.; Xu, R.N.; Jiang, P.X. Thermodynamic analysis of enhanced geothermal systems using impure $CO_2$ as the geofluid. *Appl. Therm. Eng.* **2016**, *99*, 1277–1285. [CrossRef]
46. Hu, K.; Zhu, J.; Zhang, W.; Lu, X. A selection method for power generation plants used for enhanced geothermal systems (EGS). *Energies* **2016**, *9*, 597. [CrossRef]
47. Li, M.-J.; Zhu, H.-H.; Guo, J.-Q.; Wang, K.; Tao, W.-Q. The development technology and applications of supercritical CO2 power cycle in nuclear energy, solar energy and other energy industries. *Appl. Therm. Eng.* **2017**, *126*, 255–275. [CrossRef]
48. Liao, G.; Liu, L.; Jiaqiang, E.; Zhang, F.; Chen, J.; Deng, Y.; Zhu, H. Effects of technical progress on performance and application of supercritical carbon dioxide power cycle: A review. *Energy Convers. Manag.* **2019**, *199*, 111986. [CrossRef]
49. Manente, G.; Costa, M. On the conceptual design of novel supercritical CO2 power cycles for waste heat recovery. *Energies* **2020**, *13*, 370. [CrossRef]
50. Kowalski, R.; Kuczyński, S.; Łaciak, M.; Szurlej, A.; Włodek, T. A case study of the supercritical CO2-brayton cycle at a natural gas compression station. *Energies* **2020**, *13*, 2447. [CrossRef]
51. Jankowski, A.; Całka, M.; Gierad, D.; Lombarska-Blochel, A. *Plan Gospodarki Niskoemisyjnej Dla Miast Kutno Na Lata 2015–2023*; Energoekspert Sp. z.o.o.: Kutno, Poland, 2015.
52. Ziębik, A.; Liszka, M.; Hoinka, K.; Stanek, W. *Poradnik Inwestora I Projektant Układów Wysokosprawnej Dużej Kogeneracji (N R06 0004 06)*; Politechnika Śląska: Gliwice, Poland, 2012.
53. Bujakowski, W.; Tomaszewska, B. (Eds.) *Atlas of the Possible Use of Geothermal Waters for Combined Production of Electricity and Heat Using Binary Systems in Poland*; Wydawnictwo Jak: Kraków, Poland, 2014.
54. Gładysz, P.; Ziębik, A. Complex analysis of the optimal coefficient of the share of cogeneration in district heating systems. *Energy* **2013**, *62*, 12–22. [CrossRef]

55. Świerzewski, M.; Gładysz, P. Environmental and economic assessment of a biomass-based cogeneration plant: Polish case study. *Maz. Studia Reg.* **2017**, *22*, 97–114. [CrossRef]
56. Bachu, S. Sequestration of $CO_2$ in geological media: Criteria and approach for site selection in response to climate change. *Energy Convers. Manag.* **2000**, *41*, 953–970. [CrossRef]
57. Tarkowski, R. *Geologiczna Sekwestracja $CO_2$*; Wydawnictwo Instytutu Gospodarki Surowcami Mineralnymi i Energią PAN: Kraków, Poland, 2005.
58. Kumari, W.G.P.; Ranjith, P.G. Sustainable development of enhanced geothermal systems based on geotechnical research—A review. *Earth-Sci. Rev.* **2019**, *199*, 1029–1055. [CrossRef]
59. Guterch, A.; Grad, M. Lithospheric structure of the TESZ in Poland based on modern seismic experiments. *Geol. Q.* **2006**, *50*, 23–32.
60. Sowiżdżał, A. Geothermal energy resources in Poland—Overview of the current state of knowledge. *Renew. Sustain. Energy Rev.* **2018**, *82*, 4020–4027. [CrossRef]
61. Sowiżdżał, A.; Papiernik, B.; Machowski, G.; Hajto, M. Characterization of petrophysical parameters of the Lower Triassic deposits in prospective location for Enhanced Geothermal System (Central Poland). *Geol. Q.* **2013**, *57*, 729–744. [CrossRef]
62. Šliaupa, S.; Lojka, R.; Tasáryova, Z.; Kolejka, V.; Hladík, V.; Kotulová, J.; Kucharič, L.; Fejdi, V.; Wójcicki, A.; Tarkowski, R.; et al. $CO_2$ storage potential of sedimentary basins of Slovakia, the Czech Republic, Poland and the Baltic States. *Geol. Q.* **2013**, *57*, 219–232. [CrossRef]
63. Xu, C.; Dowd, P.; Li, Q. Carbon sequestration potential of the Habanero reservoir when carbon dioxide is used as the heat exchange fluid. *J. Rock Mech. Geotech. Eng.* **2016**, *8*, 50–59. [CrossRef]
64. Bujakowski, W.; Barbacki, A.; Miecznik, M.; Pająk, L.; Skrzypczak, R.; Sowiżdżał, A. Modelling geothermal and operating parameters of EGS installations in the lower triassic sedimentary formations of the Central Poland area. *Renew. Energy* **2015**, *80*, 441–453. [CrossRef]
65. Sowiżdżał, A.; Kaczmarczyk, M. Analysis of thermal parameters of Triassic, Permian and Carboniferous sedimentary rocks in Central Poland. *Geol. J.* **2016**, *51*, 65–76. [CrossRef]
66. Gładysz, P.; Pająk, L.; Sowiżdżał, A.; Miecznik, M. $CO_2$ enhanced geothermal system for heat and electricity production—Process configuration analysis for Central Poland. In Proceedings of the ECOS 2019—The 32nd International Conference on Efficiency, Cost, Optimization, Simulation and Environmental Impact of Energy Systems, Wrocław, Poland, 23–28 June 2019.
67. Atrens, A.; Gurgenci, H.; Rudolph, V. Exergy analysis of a $CO_2$ thermosiphon. In Proceedings of the 34th Workshop on Geothermal Reservoir Engineering, Stanford, CA, USA, 9–11 February 2009.
68. Atrens, A.; Gurgenci, H.; Rudolph, V. Electricity generation using a carbon-dioxide thermosiphon. *Geothermics* **2009**, *39*, 161–169. [CrossRef]
69. Remoroza, A.I.; Doroodchi, E.; Moghtaderi, B. Modelling complete $CO_2$-EGS power generation process. In Proceedings of the New Zealand Geothermal Workshop, Rotorua, New Zealand, 21–23 November 2011.
70. Carnegie Mellon University. IECM Technical Documentation: Amine-based Post-Combustion CO2 Capture. Available online: https://www.cmu.edu/epp/iecm/iecm_docpubs.html (accessed on 15 February 2020).
71. Gładysz, P.; Świerzewski, M. Analiza energetyczna i ekologiczna elektrociepłowni zasilanej biomasą z wychwytem $CO_2$. In Proceedings of the XXIII Zjazd Termodynamików, Ustroń, Poland, 19–22 September 2017.
72. Gładysz, P.; Saari, J.; Czarnowska, L. Thermo-ecological cost analysis of cogeneration and polygeneration energy systems—Case study for thermal conversion of biomass. *Renew. Energy* **2020**, *145*, 1748–1760. [CrossRef]
73. Roussanaly, S. Calculating CO2 avoidance costs of Carbon Capture and Storage from industry. *Carbon Manag.* **2019**, *10*, 105–112. [CrossRef]
74. Kalina, J. Equipment sizing in a coal-fired municipal heating plant modernisation project with support for renewable energy and cogeneration technologies. *Energy Convers. Manag.* **2014**, *86*, 1050–1058. [CrossRef]
75. Carnegie Mellon University. Integrated Environmental Control Model (v. 11.2). Available online: https://www.cmu.edu/epp/iecm/index.html (accessed on 21 March 2020).
76. Zhao, Q. Conception and Optimization of Supercritical $CO_2$ Brayton Cycles for Coal-Fired Power Plant Application. Ph.D. Thesis, Université de Lorraine, Lorraine, France, 2018.
77. Michalski, S.; Hanak, D.P.; Manovic, V. Techno-economic feasibility assessment of calcium looping combustion using commercial technology appraisal tools. *J. Clean. Prod.* **2019**, *219*, 540–551. [CrossRef]
78. McCollum, D.L.; Ogden, J.M. *Techno-Economic Models for Carbon Dioxide Compression, Transport, and Storage & Correlations for Estimating Carbon Dioxide Density and Viscosity*; University of California: Davis, CA, USA, 2006.

79. National Fund for Environmental Protection and Water Management, Poland. Available online: http://nfosigw.gov.pl/oferta-finansowania/srodki-krajowe/programy-priorytetowe/poprawa-jakosci-powietrza-energetyczne/energetyczne-wykorzystanie-zasobow-geotermalnych/ (accessed on 10 February 2020).
80. Chemical Engineering's Plant Cost Index (CEPCI). Available online: https://www.chemengonline.com/pci-home (accessed on 20 March 2020).
81. Danish Energy Agency. Technology Data for Energy Plants for Electricity and District Heating Generation. Version Number: 0002. Available online: https://ens.dk/en/our-services/projections-and-models/technology-data/technology-data-generation-electricity-and (accessed on 15 February 2020).
82. Gładysz, P. System Analysis of an Integrated Oxy-Fuel Combustion Power Plants. Ph.D. Thesis, Silesian University of Technology, Gliwice, Poland, 25 May 2015.
83. Gatti, M.; Martelli, E.; Di Bona, D.; Gabba, M.; Scaccabarozzi, R.; Spinelli, M.; Viganò, F.; Consonni, S. Preliminary performance and cost evaluation of four alternative technologies for post-combustion CO2 capture in natural gas-fired power plants. *Energies* **2020**, *13*, 543. [CrossRef]
84. International Renewable Energy Agency. *Renewable Power Generation Costs in 2018*; International Renewable Energy Agency: Abu Dhabi, UAE, 2019.
85. Feron, P.H.M. (Ed.) *Absorption-Based Post-Combustion Capture of Carbon Dioxide*; Series in Energy; Woodhead Publishing: Shaston, UK, 2016.
86. Tamaryn, N. A Survey of Key Technological Innovations for the Low-Carbon Economy. 2017. Available online: https://www.oecd.org/env/cc/g20-climate/collapsecontents/Imperial-College-London-innovation-for-the-low-carbon-economy.pdf (accessed on 6 January 2020).
87. Bui, M.; Adjiman, C.S.; Bardow, A.; Anthony, E.J.; Boston, A.; Brown, S.; Fennell, P.S.; Fuss, S.; Galindo, A.; Hackett, L.A.; et al. Carbon capture and storage (CCS): The way forward. *Energy Environ. Sci.* **2018**, *11*, 1062–1176. [CrossRef]
88. Wertich, V.; Tiewsoh, L.S.; Tiess, G. CHPM2030 Deliverable D5.2: Economic Feasibility Assessment Methodology. *Zenodo* **2018**. Available online: https://zenodo.org/record/1405865 (accessed on 29 April 2020).
89. Guinot, F.; Meier, P. Can unconventional completion systems revolutionise EGS? A critical technology review. In *SPE Europec Featured at 81st EAGE Conference and Exhibition*; Society of Petroleum Engineers: Dallas, TX, USA, 2019.
90. Wilberforce, T.; Baroutaji, A.; El Hassan, Z.; Thompson, J.; Soudan, B.; Olabi, A.G. Prospects and challenges of concentrated solar photovoltaics and enhanced geothermal energy technologies. *Sci. Total Environ.* **2019**, *659*, 851–861. [CrossRef] [PubMed]
91. Zhang, Y.; Zhao, G.F. A global review of deep geothermal energy exploration: From a view of rock mechanics and engineering. *Geomech. Geophys. Geo-Energy Geo-Resour.* **2020**, *6*, 4. [CrossRef]
92. Ahn, Y.; Bae, S.J.; Kim, M.; Cho, S.K.; Baik, S.; Lee, J.I.; Cha, J.E. Review of supercritical CO2 power cycle technology and current status of research and development. *Nucl. Eng. Technol.* **2015**, *47*, 647–661. [CrossRef]
93. International Renewable Energy Agency. Biomass for power generation. In *Renewable Energy Technologies: Cost Analysis Series*; IRENA: Abu Dhabi, UAE, 2012; Volume 1.
94. Consoli, C. *Perspective. Bioenergy and Carbon Capture and Storage*; Global CCS Institute: Melbourne, Australia, 2018.